Aspects of QCD Phase Transition with Reaction-Diffusion Equations

By

Srikumar Sengupta

PHYS07200604017

Institute of Physics, Bhubaneswar

A thesis submitted to the

Board of Studies in Physical Sciences

In partial fulfillment of requirements

For the Degree of

DOCTOR OF PHILOSOPHY

of

HOMI BHABHA NATIONAL INSTITUTE

April, 2016

STATEMENT BY AUTHOR

This dissertation has been submitted in partial fulfillment of requirements for an advanced degree at Homi Bhabha National Institute (HBNI) and is deposited in the Library to be made available to borrowers under rules of the HBNI. Brief quotations from this dissertation are allowable without special permission, provided that accurate acknowledgement of source is made. Requests for permission for extended quotation from or reproduction of this manuscript in whole or in part may be granted by the Competent Authority of HBNI when in his or her judgment the proposed use of the material is in the interests of scholarship. In all other instances, however, permission must be obtained from the author.

Date:- April 1, 2016. (Srikumar Sengupta)

CERTIFICATE

This is to certify that the thesis entitled "Aspects of QCD Phase Transition with Reaction-Diffusion Equations", which is being submitted by **Mr. Srikumar Sengupta**, in partial fulfillment of the degree of **Doctor of Philosophy in Physics** of **Homi Bhabha National Institute** is a record of his own research work carried by him. He has carried out his investigations on the subject matter of the thesis under my supervision at **Institute of Physics, Bhubaneswar**. To the best of our knowledge, the matter embodied in this thesis has not been submitted for the award of any other degree.

Signature of the Candidate **Signature of the Supervisor**

Srikumar Sengupta
Institute of Physics
Bhubaneswar

Dr. Ajit M. Srivastava
Professor
Institute of Physics
Bhubaneswar

Date:- April 1, 2016.

DECLARATION

I, Srikumar Sengupta, hereby declare that the investigations presented in the thesis have been carried out by me. The matter embodied in the thesis is original and has not been submitted earlier as a whole or in part for a degree/diploma at this or any other Institution/University.

Date: April 1, 2016. (Srikumar Sengupta)

To My Parents

Contents

Acknowledgement

This thesis is the culmination of an extended research effort under a total of three advisors (!!), which, I believe, is a record of some sort. It is, therefore, only natural that the present work owes much to many people. In what follows below is a list, exhaustive to the extent my memory allows me to be so, of all those who have contributed to it in a myriad of ways, direct or indirect. I apologise in advance for any inadvertent/unintentional omissions.

My parents - although none of my parents is around to see this day, I believe it is only because of their blessings that I could make this long and exasperating journey. Thank you, dear ma and baba, for being what you were. Thank you for instilling in me a love for academics. If there are certain values that I live by, it is because I have imbibed them from you. The failings are, of course, mine.

My thesis advisor Ajit - it is impossible to summarize the role played by this man in resurrecting my research career. He literally lifted it out of doldrums to make this thesis happen. In these days when one is oftentimes reminded of Billy Joel's immortal lyrics - "'Honesty - is such a lonely word, everyone is so untrue. "'here is a man who stands as a living rebuttal of it. I restrict myself to an assessment of Ajit as a human being only because I am too ignoramus to comment on his physics. All that I can say is I have always been amazed at his grasp of physics in its entirety and I have always wondered as to how he manages to pose the most searching of questions even in talks delivered on areas far removed from his own expertise. Also, it is a pleasure to recall the cheerful hospitality with which ma'am (Shikha) received us at her place on so many occasions. Thank you so much, ma'am.

My immediate family members - my elder brother, sister-in-law and niece - for their concern, encouragement, and moral support for everything that I do, the presnt work included. I should also mention in the same breath my friend Anwesha who has been a pillar of support for over a decade now. It is only because of her, together with my dada and boudi, that I could soldier on and indulge in the luxury of continuing research with the odds heavily set against me. Otherwise, I would have had to call it quits a long time back. I take this opportunity to express my gratitude to my extended family as well, which includes Surjo-da, Babla-da, boudi, my maternal uncles, mami,

and my cousin sisters - they have always wished me well.

Another person who has been with me through thick and thin, rain or shine, is my friend Anupam. A wise head on young shoulders, Anupam has over the years ably guided me through many a difficult decision. The guy always makes me see light at the end of a tunnel, no matter how long and dark the tunnel is! And, I could go on and on if I am to recount all the help that I have received from him in matters related to the computer. THANK YOU, dear Anupam, for everything that you have done, and continue to do, for me.

The help I have received from three very special people - Partho, Arpan and Shreyansh - is too big for words. Coming from a different background as I did, I was pleasantly surprised at the sense of oneness and the feeling of camaraderie that exist in the astroparticle physics group at IoP. This, I guess, is something that the group members have imbibed from the group mentor Ajit. In these days of unabashed selfishness, such selflessness is rare indeed. One request to all three of them - do stay the way you are; please do not change;- the world will be the poorer if you do. A special word of thanks goes to Sreya as well for her sumptuous meals at her place - she is indeed an out-of-the-world cook. A word of apology is in order too - I routinely snatched Partho away from her at hours which were rightfully hers; sorry, Sreya.

I am thankful to Rajarshi Ray of Bose Institute, as well as Partho, for their introductory lectures on QGP. These lectures indeed eased my way into an allien territory. My thanks go to Abhishek as well for sharing with me the latex file of his thesis; this made thesis writing so much easier.

The computer has always been my Achilles heel and a host of people over the years - Anupam, Tanay, Soumen, Probodh (he helped me communicate my first paper), Souvik, Sumaloy (they helped me communicate my second paper), Partho, Arpan, Shreyansh - have helped me face and survive this horror of horrors . I thank them all for ungrudgingly bearing the burden that is me.

I express my sincerest gratitude to my late advisor Prof. Alok Kumar for initiating me into research. He gave me independence of work and allowed me to work at my own pace. I owe my two papers in string theory to him only. I am also grateful to Prof. Sudipto Mukherjee for agreeing to be my advisor at the untimely death of Alok's. I thank Prof. Mukherjee for supporting my extension for three years after

Alok's death.

It is a pleasure to remember fondly my happy association with my onetime stringy co-dwellers - Sandip, Tanay, Sudipto (Pal Chaudhuri), Sankha, Sachin, Souvik, Anirban, Swarnendu, Subir, Kamal, Chandra, and Sayan. I specially prize the bonding I share with Sandip, Tanay, Sudipto, Sachin, and Souvik.

I shall be failing in my duty if I do not mention a few others to whom I am indebted in one way or the other, such as - Hara, Venky, Anand, Ajay, Umananda, Sougata, Nabyendu, Poulomi, Jim, Ram Babu, Ravan Babu, and Duryodhan Babu.

I owe a special word of thanks to Bidisha. She allowed me to use her desk and computer on all my visits to IoP. This must have inconvenienced her but she never complained and never made me feel obligated. Thank you Bidisha for this act of magnanimity.

Another person who deserves special mention is Sabyasachi. A ruthless opponent at the chess-board, he is otherwise a kind soul and a great company. Back in Kolkata, I always miss the long-drawn chess battles and the longer "adda" sessions that I have with him here.

My friends back in Kolkata - Papu, Tapa, Subhendu, Kutush, Pantha - helped me tide over many a crisis at home. No word of thanks, however sincere, is good enough for them. I am thankful to Bappa for sorting out troubles with my laptop. Shikha took great care of my mother and I can never thank her enough for that. To Nazrul I owe very special thanks - but for him I would have never finished my Ph.D.

Last but by no means the least - I thank all the dogs - back home, in my locality, and here at IoP - for adding 'color' and 'flavor' to my life. I love you all.

Date: April 1, 2016. **Srikumar Sengupta**

Synopsis

Quantum chromodynamics predicts that at extreme conditions of baryon density and /or temperature there should be a deconfinement of quarks and gluons, and hadrons should undergo a phase transition to quark-gluon plasma (QGP). In the hot Big-Bang model of the universe, at very early stages, when the age of the universe was 10^{-5} sec and the temperature was 10^{12} K, the universe consisted of a hot plasma of elementary particles e.g. quarks, gluons, etc. There is mounting evidence that ultra-relativistic collision of two heavy nuclei results in the production of an extremely dense, thermalized, system of quarks and gluons, just like the above stage of the universe.

These experiments make it possible to explore the interesting phases and phase transitions of QCD. There are two important phase transitions associated with QCD. One is associated with chiral symmetry breaking and the other is the confinement-deconfinement (C-D) transition. Chiral symmetry is a very important symmetry of QCD which arises in the vanishing mass limit of certain quark flavors, in particular the u and the d (for two-flavor chiral symmetry). This leads to decoupling of the left and the right handed components of the massless quarks leading to $SU(2)_L \times SU(2)_R$ global symmetry for the QCD Lagrangian. However, low energy hadronic spectrum does not exhibit parity doubling of hadronic spectrum as one would have expected from this chiral symmetry. This is only possible if the vacuum of QCD does not respect chiral symmetry. In view of the fact that hadronic spectrum does exhibit multiplet structure of SU(2) isospin (again, for the two flavor case), one is led to the conclusion that the chiral symmetry $SU(2)_L \times SU(2)_R$ is spontaneously broken to its diagonal subgroup $SU(2)_{isospin}$. The three Goldstone bosons expected from this are regarded to be the three pions. However, pions are not massless; they have nonzero masses arising from nonzero masses of quarks. Thus chiral symmetry is also explicitly broken. A simple phenomenological model which implements the idea of chiral symmetry breaking is the linear sigma model with the Lagrangian

$$\mathcal{L} = \frac{1}{2}\left[(\partial_\mu \sigma)^2 + (\partial_\mu \pi)^2\right] - V(\sigma, \pi) + H\sigma, \tag{0.1}$$

with the potential $V(\sigma, \pi)$ describing the self-interaction of the scalars and is given

by

$$V(\sigma,\pi)=\frac{\mu^2}{2}(\sigma^2+\pi^2)^2+\frac{\lambda}{24}(\sigma^2+\pi^2)^4. \tag{0.2}$$

The $H\sigma$ term makes the vacuum manifold non-degenerate giving rise to a non-zero mass for pions.

The other phase transition in QCD, namely the confinement-deconfinement transition, is associated with the liberation of color degrees of freedom (from being confined inside hadrons), at high temperature/baryon density. The order parameter for the C-D transition is taken to be the thermal expectation value of the Polyakov loop. The Polyakov loop is defined as

$$L(x)=\frac{1}{N}Tr\left[\mathbf{P}exp\left(ig\int_0^\beta A_0(\vec{x},\tau)d\tau\right)\right].$$

Its thermal expectation value is related to the free energy of a static test quark by

$$\langle L(\vec{x})\rangle = e^{-\beta\Delta F}.$$

The two phases of QCD are distinguished as follows:

Confining Phase:- Quarks are confined. Thus, for an isolated static test quark one expects, $\Delta F\to\infty\Rightarrow\langle L(x)\rangle=0$.

Deconfining Phase:- The color degrees of freedom are liberated, so isolated test quarks can exist. This means, ΔF is finite $\Rightarrow\langle L(x)\rangle\neq 0$.

For the dynamics of the order parameter $l(x)$ which is the expectation value of the Polyakov loop, we use the following effective Lagrangian density [1]

$$\mathcal{L}=\frac{N}{g^2}|\partial_i l|^2T^2-V(l), \tag{0.3}$$

where

$$V(l)=\left(-b_2|l|^2+b_3(l^3+(l^*)^3)+|l|^4\right)b_4T^4. \tag{0.4}$$

l has the value zero at low temperatures and the potential has only one minimum at $l=0$. For $T>T_c$, $l(x)$ has a non-zero vacuum expectation value l_0. ($V(l)$ has three degenerate $Z(3)$ vacua. However, we are not interested in this $Z(3)$ structure; hence we only focus on one vacuum at real $l=l_0$).

Earlier it used to be believed that the quark-hadron transition is of first order even at low chemical potential (as in the early universe). This led to a very important proposal by Witten [2] about the possibility of formation of quark nuggets due to the concentration of quarks by moving phase boundaries at the quark-hadron transition. Should quark-hadron transition be first order, the dynamics of first order transition necessarily has important implications for heavy-ion collisions [3]. However, lattice results show that the quark-hadron transition is not first order; rather, it is a cross-over for low chemical potential. Thus, the earlier results associated with a first order QCD transition, potentially important as they were, became irrelevant.

One notes here that as regards the dynamics of phase transition, the most important difference between a first order transition and a cross-over (or a continuous transition) is the presence of an interface for the first order transition case which separates the two phases. The transition for a first order case is completed by nucleation of bubbles which expand. The moving bubble walls (phase boundaries) lead to physical phenomena, such as non-trivial scattering of quarks, local heating, etc., which are qualitatively different from the case of cross-over or a continuous transition.

It turns out that the presence of moving interfaces is more generic, and not necessarily restricted to the case of first order transitions. Such situations routinely arise in the study of so called *reaction-diffusion equations* [4,5]. In this thesis we demonstrate such solutions for chiral phase transition and confinement-deconfinement (C-D) transition in QCD even when the underlying transition is a cross-over or a continuous transition. The only difference between the field equations in relativistic field theory case and the reaction-diffusion case is the absence of a second order time derivative in the latter case. The correspondence between the two cases can be established in the presence of a strong dissipation term leading to a dominant first order time derivative term. We also show that the required boundary conditions for the existence of such slowly moving propagating fronts naturally arise in relativistic heavy-ion collision experiments (RHICE).

For discussing reaction-diffusion equations, we start with the diffusion equation,

$$\frac{\partial c}{\partial t} = D\,\nabla^2\,c. \tag{0.5}$$

This has 1-d solution,

$$c\,(\,x,\,t) = \frac{c_0}{2\,(\pi\,D\,t)^{1/2}}\,e^{-\,x^2\,/4\,D\,t}. \tag{0.6}$$

It is known that this has no traveling wave solution. The reaction-diffusion equation is written as follows,

$$\frac{\partial\,c}{\partial\,t} = f\,+\nabla\,\cdot\,(\,D\,\nabla\,c\,), \tag{0.7}$$

where f is the reaction term denoting interaction of the variable c. Remarkably, this equation has traveling wave solutions.

QCD transitions in RHICE are cross-over transitions. So there is no phase boundary in such transitions as in a first order phase transition. We show that moving interfaces arise here due to correspondence with the reaction-diffusion equations with appropriate boundary conditions. The field equation for the case of spontaneous chiral-symmetry-breaking transition for the two flavor case O(4) field $\phi = (\sigma, \vec{\pi})$ as the chiral order parameter is

$$\ddot{\phi} - \bigtriangledown^2\phi + \eta\dot{\phi} = -4\lambda\phi^3 + m(T)^2\phi + H,$$

$$m(T)^2 = \frac{m_\sigma^2}{2}(1 - \frac{T^2}{T_c^2}). \tag{0.8}$$

Here, ϕ is taken along the σ direction.

For establishing direct correspondence with a reaction-diffusion equation, we first use the approximations that H=0, and η is large and time independent, so that we can neglect the $\ddot{\phi}$ term. We rescale the variables as, $x \to m(T)x$, $\tau \to \frac{m(T)^2}{\eta}\tau$, and $\phi \to 2\frac{\sqrt{\lambda}}{m(T)}\phi$.

With this, the field equations simplify to,

$$\dot{\phi} = \bigtriangledown^2\phi - \phi^3 + \phi. \tag{0.9}$$

This equation in one dimension with $\bigtriangledown^2\phi = d^2\phi/dx^2$, is exactly the same as the reaction-diffusion equation known as the Newell-Whitehead equation. The analytical solution with boundary conditions $\phi = 0$ and 1 at $x \to \pm\infty$ is,

$$\phi(z) = [1 + exp(z/\sqrt{2})]^{-1}, \tag{0.10}$$

where $z = x - v\tau$. v is the velocity of the front $= 3/\sqrt{2}$.

For the chiral symmetry breaking transition in relativistic heavy-ion collisions, the boundary conditions are: (1) At the center, $T > T_c \Longrightarrow$ the chiral field takes chirally (approximately) symmetric value.
(2) At large r, $T < T_c \Longrightarrow$ the chiral field takes symmetry broken value. We take the same initial field-profile even when the temperature at the center becomes $T_0 < T_c$. Once T_0 is reached, we take T_0 to be constant over the range of the profile of ϕ.

With these boundary conditions the analytical solution is,

$$\phi(z) = \xi[1 + exp(\frac{m(T)}{\sqrt{2}}(x - v\tau))]^{-1}, \tag{0.11}$$

where $\xi = \frac{m(T)}{2\sqrt{\lambda}}$ is the VEV of ϕ (for $H = 0$) and $v = \frac{3m(T)}{\eta\sqrt{2}}$.

Next, we consider the confinement-deconfinement transition during early thermalization stage. For RHICE, at very early stages, Bjorken scaling with longitudinally expanding plasma is a very good approximation. The dissipation term is very strong during the early stages. We study the C-D transition using the expectation value of the Polyakov loop order parameter.

The Lagrangian density is as given in Eqn(3),(4). We take real l and neglect the second order time derivative (for large dissipation case).

The variables are scaled as, $x \to gT\sqrt{\frac{b_4}{2N}}x$, and $\tau \to \frac{b_4 g^2 T^2}{2\eta N}\tau$. The field equation for real $l(x)$, written as $\phi(x)$, is,

$$\dot{\phi} = \bigtriangledown^2\phi + \phi(b_2 + b_3\phi - \phi^2). \tag{0.12}$$

This is the same as another reaction-diffusion equation known as the Fitzhugh-Nagumo equation which is used in population genetics.

We have numerically solved the field equations for both cases, namely chiral phase transition and C-D transition, with realistic time dependence of dissipation as well as temperature. We have shown that propagating fronts exist in both cases which dramatically change the dynamics of phase transition, almost making it like a first order transition [6].

In the second work we revisit the issue of formation of so called disoriented chiral condensate (DCC) [7]. DCC corresponds to formation of an extended region, where the chiral field is misaligned from the true vacuum. This possibility was investigated

extensively some time ago and it was proposed that DCC may form in large multiplicity hadronic collisions or in heavy-ion collisions [8–11]. A large DCC domain would lead to spectacular signatures such as coherent emission of pions which can be detected [9] as anomalous fluctuations in the ratio R of neutral pions to all pions. However, even after extensive experimental search for DCC, no clear signals were found for its formation. Alhough it was generally agreed that in heavy-ion collisions, chiral-symmetry-breaking transition will necessarily lead to formation of many DCC domains, the expected size of such DCC domains was too small, and their numbers too large in any given event, that standard DCC signals were washed out. Indeed, from this perspective, heavy-ion collisions were not ideally suited for the detection of DCC. With a large volume system undergoing chiral-symmetry-breaking transition, multiple DCC domains necessarily result, and a clean signal of coherent pion emission becomes very unlikely. In comparison, a pp collision, involving a small volume system, could, in principle, lead to a single DCC domain.

Next, we reconsider the issue of DCC formation in the context of (very) large multiplicity pp collisions at LHC energies. Some of the earliest suggestions for DCC formation were actually made in the context of high multiplicity hadronic collisions. One would expect that a pp collision, with a small volume system, could lead to a single DCC domain with a relatively cleaner signals of coherent pion emission. However, at previously attained energies, it was never clear whether the necessary condition for DCC formation, namely, an intermediate stage of chiral-symmetry-restoration, was ever achieved. Further, even if chiral symmetry was restored, the resulting DCC domains would have been too small, of the order of a few fm^3, in view of rapid roll-down of the chiral field to the true vacuum. This will lead to only few pions from which a clear signal, say of neutral to charged particle ratio, would be hard to detect.

The conditions for chiral symmetry restoration seem much more favorable for the very high multiplicity pp collisions at LHC energy. Indeed there are strong indications that several signals which have been attributed to a thermalized medium undergoing hydrodynamic expansion in heavy-ion collisions, may be present in such high energy pp collisions [12]. It is entirely possible that the energy density/temperature of such a medium may cross the chiral transition temperature. This will take care of the

requirement of an intermediate stage of chiral symmetry restoration for DCC formation. We show in this paper that the problem of rapid roll down of the chiral field to true vacuum is alleviated due to a rapid three dimensional expansion of the system which makes reaction-diffusion equation applicable for governing the dynamics of the chiral field for this system (with appropriate boundary conditions which, as we show, naturally arise in these events). The expanding system leads to a DCC domain which stretches and becomes larger due to expansion, without the chiral field significantly rolling down (due to specific properties of the solutions of reaction-diffusion equations). Eventually one gets a large DCC domain the subsequent decay of which should lead to coherent pion emission.

To conclude, we have used the techniques of reaction-diffusion equations to show the existence of well defined traveling front solutions, which are very similar to the phase boundaries for a first order transition case, even though the relevant QCD transitions here are of second order, or a cross-over. During the time when dissipation dominates, we see that the transition proceeds by a slow-moving front, and may take several fm time to complete, leading to a long lasting mixed phase stage. This should have a bearing on calculations of various signals of QGP for RHICE, e.g. production of thermal photons and di-leptons, J/ψ suppression, quark scattering (possibly leading to baryon rich clusters) and especially elliptic flow which develops mostly during the early stages. We have also considered the possibility of formation of disoriented chiral condensates (DCC) in high multiplicity pp collisions at LHC energy. We show that the interior of such a rapidly expanding system is likely to lead to the formation of a single large domain of DCC which has been a subject of intensive search in earlier experiments. We argue that large multiplicity pp collisions naturally give rise to the required boundary conditions for the existence of slowly propagating front solutions of reaction-diffusion equation with the resulting dynamics of the chiral field leading to the formation of a large DCC domain.

Bibliography

[1] O. Scavenius, A. Dumitru, and J. T. Lenaghan, Phys. Rev. **C66**, 034903 (2002); R.D. Pisarski, Phys. Rev. **D62**, 111501R (2000).

[2] E. Witten, Phys. Rev. **D 30**, 272 (1984).

[3] S. Digal and A.M. Srivastava, Phys. Rev. Lett. **80**, 1841 (1998).

[4] A.G. Nikitin, T.A. Barannyk, Central European Journal of Mathematics 2(5), 840 (2004); B. Bradshaw-Hajek, *Reaction-diffusion equations for population genetics*, PhD thesis, School of Mathematics and Applied Statistics, University of Wollongong, 2004, http://ro.uow.edu.au/theses/201;

[5] *Progress in Nonlinear Differential Equations and Their Applications*, Editor H. Brezis, Springer Basel AG, Switzerland (2004).

[6] Partha Bagchi, Arpan Das, **Srikumar Sengupta** and Ajit M. Srivastava, Phys. Rev. **C92**, (2015) 3, 034902; arXiv:1507.01015

[7] Partha Bagchi, Arpan Das, **Srikumar Sengupta** and Ajit M. Srivastava, (arXiv:submit/1339579 [nucl-th], submitted for publication to Phys. Rev.C.).

[8] A. A. Anselm, Phys. Lett. **B217** (1989) 169; J.-P. Blaizot and A. Krzywicki, Phys. Rev. **D46** (1992) 246.

[9] J.D. Bjorken, K.L. Kowalski and C.C. Taylor, in *Results and Perspectives in Particle Physics 1993*; Proceedings of the 7th Rencontres de Physique de la Vallee d'Aoste, La Thuile, Italy, 1993, edited by M. Greco (Editions Frontieres, Gif-sur-Yvette, France, 1993).

[10] J. P. Blaizot and D. Diakonov, Phys. Lett. **B315** (1993) 226.

[11] K. Rajagopal and F. Wilczek, Nucl. Phys. **B399** (1993) 395; *ibid* **B404** (1993) 577.

[12] P. Ghosh, S. Muhuri, J.K. Nayak, and R. Varma J.Phys. **G 41**, 035106 (2014); I.B. Bashir, R.A. Bhat, and S. Uddin, arXiv: 1502.04185.

List of Publications

1. **Published/Accepted for publication**

   (a) *****_Reaction-diffusion equation for quark-hadron transition in heavy-ion collisions_

   Partha Bagchi, Arpan Das, **Srikumar Sengupta** and Ajit M. Srivastava
   Phys. Rev. **C92**, (2015) 3, 034902; arXiv:1507.01015

   (b) *****_Possibility of formation of a disoriented chiral condensate in pp collisions at energies available at the CERN Large Hadron Collider via the reaction-diffusion equation_

   Partha Bagchi, Arpan Das, **Srikumar Sengupta** and Ajit M. Srivastava
   Phys.Rev. **C93**, (2016) no.2, 024914; arXiv:1508.07752

   (c) _Brane Solutions in Time Dependent Backgrounds in D = 11 Supergravity and in Type II String Theories_

   Srikumar Sen Gupta
   Int.J.Mod.Phys. A23 (2008) 2525-2540

   (d) _Some new light-cone time dependent solutions in deformed pp-wave backgrounds_

   Srikumar Sen Gupta
   JHEP 05, 038 (2014)

(*****) indicates the papers on which this thesis is based.

List of Figures

Chapter 1

Introduction

1.1 The Microcosmos

The quest for the ultimate building blocks of nature can be traced back to the ancient notion of the five elements - earth, water, air, fire, and ether - that were supposed to be the basic constituents of the world about us. Several hundred centuries later, thanks to the efforts of the chemists, came the notion of the chemical elements - molecules and atoms -and finally, with physics taking over, of the particles within the atoms, and even within the nucleus. The motivation behind the long and arduous journey has been the hope that should one be able to identify one day the truly elementary players - hopefully of only a few distinct types - and learn the rules they play by, physics can perhaps be reduced to a straightforward but possibly very difficult exercise.

We have not arrived at the end of our search and perhaps we never will. Much has been learnt but one suspects that much more remains to be learnt; every stride forward makes us realize, much to our dismay and delight, that there is an expanding frontier of ignorance, and there is universal agreement that the grand pattern still very definitely eludes us. In a lighter vein, this has kept physicists from going out of business! Our experience so far has been what is thought to be elementary today has, mostly, yielded substructure on further probings at higher energies. Thus, the underlying motivation for constructing increasingly more elaborate accelerating machines is to probe the subnuclear domain using very short wavelength, high-energy incident particles. At the present level of energies available and the resolution accruing therefrom, the smallest units of matter seem to be the leptons and the quarks, both of which are spin half fermions. The leptons come in six varieties and can be listed as

$$\text{Leptons}: \quad (\nu_e, e^-), \quad (\nu_\mu, \mu^-), \quad \text{and} \quad (\nu_\tau, \tau^-).$$

Since all particles have their antiparticles, so, including the antiparticles of the above list, we have a total of twelve leptons. Now, coming to the quarks, we have six

different types or flavors of them. They are : up (u), down (d), charm (c), strange (s), top (t), and bottom (b). We can list them as

$$\text{Quarks :} \qquad (u,d), \quad (c,s), \quad \text{and} \quad (t,b).$$

Each of the six different quark flavors, in turn, comes in three 'colors', and, as with the leptons, counting the antiparticles, we have a total of $(6\times3\times2) = 36$ quarks. The 12 leptons and the 36 quarks, give us a grand total of 48 matter particles, which, therefore, constitute the fundamental matter spectrum of the Standard Model of particle physics.

Now, if we aim at a complete understanding of nature, it is important that we not only know what its fundamental constituents are, but also the forces which operate among them. Otherwise, we would never understand what holds the quarks together, or what binds the electrons to the nucleus to form an atom, or, on a more mundane level, why our planet earth remains enslaved to the sun in a tireless annual motion round it through ages. Within limitations of our current knowledge, there are just four basic forces known to physics. They are, in order of increasing strength, - 1) gravitational, 2) weak, 3) electromagnetic, and 4) strong. Quantum theory suggests that all these forces are mediated by the exchange of a particle or field mediator. The graviton is the mediator of the gravitational force, the electromagnetic force is mediated by the photon, the strong force by the gluons and there are eight varieties of them, and the weak force by the intermediate vector bosons $W^{\pm}$ and Z^0. All field mediators are bosons and while the graviton, the photon and the gluons are all massless, spontaneous symmetry breaking lends masses to the carriers of the weak force with the Higgs boson playing a crucial role in the process. The Higgs particle has proven to be stubbornly elusive for long but recent runs of the LHC at CERN have thankfully, one hopes, confirmed the existence of a Higgs-like boson. The Standard model thus has twelve force carriers : the eight gluons, the $W^{\pm}$, the Z^0, and the photon. Together with the graviton, which we have not mentioned above because gravity, important though it is, falls outside the scope of the Standard model, we have a total of thirteen force carriers. Fortunately for us, the photon, the graviton, the Z^0, and the gluons are all their own antiparticles, whereas W^+ is the antiparticle of W^- and vice-versa. The 48 matter particles, the 13 force mediators and the elusive Higgs, therefore, comprise the microcosmos of nature [1].

In this thesis we shall be mainly concerned with phenomena in which quarks and gluons will be the major players. This being so, we next proceed to talk about the players and the games they play in a little more detail.

1.2 QCD : an overview

The strongly interacting particles, collectively called hadrons, are made up of

quarks, antiquarks, and gluons.These, then, are the fundamental particles relevant to QCD. As already mentioned quarks are spin half fermions characterized by six flavor degrees of freedom (u, c, t, d, s, b). The first three have charge $+\frac{2}{3}e$ and the remaining have $-\frac{1}{3}e$. Quarks typically have two types of masses :

i) the current quark mass which is the mass of a quark in the absence of confinement and is about 2, 5 MeV for u, d quarks respectively and 173 GeV for a t quark. This is the mass that enters in the QCD Lagrangian.

ii) the constituent quark mass which is the effective mass of a quark confined in a hadron and is reflective of the zero-point energy of the quark in the confining potential. The constituent mass contribution for quarks is of the order of 330 MeV for u, d quarks. The concept of constituent quark mass is, however, superfluous for a t quark because till date one does not know of any hadron involving the t quark.

Quarks also have an internal quantum number called color. The color charge was first postulated to explain the existence of the $\triangle^{++}$ state with spin $+\frac{3}{2}$. The state is symmetric in quark flavor and spin indices; so is the space part of the wave function (L=0). Thus, without the existence of an additional quantum number, this fermionic wave function would be totally symmetric, a possibility disallowed for fermions by the Pauli principle. Hence an additional degree of freedom, called color, was introduced to distinguish the otherwise identical quarks : each quark flavor carries three different color charges, red, green, and blue. The color wave function is completely antisymmetric and all known hadrons are color singlets. Thus, the color quantum number is hidden - a fact known as color confinement which is consistent with the non-existence of a free quark (i.e. a color triplet state) or such systems as (qq), ($\bar{q}$qq) etc. Quarks appear in nature only in combination as hadrons which in turn can be classified into :

i) Mesons : These are (q$\bar{q}$) systems with integral spins (i.e. bosons).

ii) Baryons : They are (qqq) systems with half integer spins (i.e. fermions).

One of course has to consider the antiparticles of the above two groups too. Since all quarks carry baryon number $+\frac{1}{3}$ and antiquarks carry baryon number $-\frac{1}{3}$, so baryons have integer baryon number while mesons have baryon number zero.

In the light of the above facts any theory purporting to describe the interaction of quarks must have the following features :

1. The interaction should result from the color charges of quarks just as electromagnetic interactions arise from electric charges. As in QED, here too it is postulated that quarks interact among themselves through the exchange of a gluon much as the photon mediates electromagnetic interaction. Further, taking clue from the success of QED, one demands that the theory be a gauge theory respecting local gauge invariance. This in turn requires that the gluons, which are the field quanta of the gauge field, be massless. Color confinement should then emerge as a natural consequence of the theory.

2. Insights derived from deep-inelastic scattering experiments involving leptons

and nucleons show that quarks are almost free inside hadrons and this is amply borne out by the success of Bjorken scaling [2] and the parton model [3]. We, therefore, need a theory with a running coupling constant $\alpha_s(q^2)$ as a function of the amount of momentum transfer q^2. It goes to zero for large q^2 leading to asymptotic freedom and becomes large for small q^2. In four dimensions only a non-Abelian gauge theory of Yang-Mills type has this kind of behavior.

The theory which meets the above two requirements and describes the interaction of quarks arising from the exchange of gluons is called quantum chromodynamics (QCD). The internal symmetry group is the $SU(3)_c$ group with the quarks transforming under the 3-dimensional fundamental representation of the group. Since the $SU(3)_c$ group has eight generators, we need eight gauge fields $A^a{}_\mu$, $a = 1, ...8$. So we have 8 gluons, all massless, corresponding to these 8 gauge fields and they transform under the adjoint representation of $SU(3)_c$. In sharp contrast to QED, the gluons themselves carry color charge ; so, unlike photons, they couple not only to quarks but to other gluons as well which makes QCD much more complicated than QED but also much richer. This is also the hallmark of any non-Abelian gauge theory.

Let us now turn to some mathematical detail of the theory. We begin with the QCD Lagrangian

$$\mathcal{L} = -\frac{1}{4} G^a_{\alpha\beta} G_a^{\alpha\beta} + \sum_\alpha \bar{\psi}_\alpha \left(i\gamma^\mu D_\mu - m_\alpha \right) \psi_\alpha, \tag{1.1}$$

where $\alpha = u, d, c, s, t, b$ is the flavor index for quarks, and D_μ, the covariant derivative, is given by

$$D_\mu = \partial_\mu - igT_a A^a_\mu, \tag{1.2}$$

where T_a are the generators of $SU(3)$ in the fundamental representation. They satisfy the Lie algebra of $SU(3)$

$$[T^a, T^b] = if^{abc} T^c \tag{1.3}$$

where f^{abc} are the antisymmetric structure constants.
$G_{\alpha\beta}$ is the gluonic field strength tensor, which is related to the commutator of covariant derivative as

$$\Big[D_\alpha, D_\beta \Big] = igG_{\alpha\beta} \equiv igT_a G^a_{\alpha\beta}\,, \tag{1.4}$$

where

$$G^a_{\alpha\beta} = \partial_\alpha A^a_\beta - \partial_\beta A^a_\alpha + g f^{abc} A^b_\alpha A^c_\beta\,. \tag{1.5}$$

Under $SU(3)$ rotations U, the fields transform as

$$\psi \to \psi' = U\psi, \tag{1.6}$$

and

$$T_a A^a_\mu \to T_a A^{a\,\prime}_\mu = U T_a A^a_\mu U^{-1} - i\Big(\partial_\mu U \Big) U^{-1}. \tag{1.7}$$

It is worth mentioning in this context that the QCD Lagrangian contains gluonic self-interaction terms like

$$g\partial_\nu A^a_\mu f^{abc} A^{\mu b} A^{\nu c} \quad \text{and} \quad g^2 f^{abc} f^{alm} A^b_\mu A^c_\nu A^{\mu l} A^{\nu m}.$$

Physically, gluons carry color charge, so they can interact with both quarks and gluons with the exchange of other gluons. This feature is also brought out by three point and four point vertices for gauge bosons in the corresponding Feynman diagrams. This can be seen rather directly if one constructs the Noether charge for the gluon field. Such self interacting gauge fields are a signature of all gauge theories with a non-Abelian gauge group. This stands in contradistinction to gauge theories with an Abelian gauge group such as QED, with $U(1)$ gauge group, the gauge bosons (i.e. photons) of which carry no charge and hence cannot self-couple.

Fortunately for us QCD is a renormalizable theory. A necessary consequence of renormalizability is that various parameters studied in the theory (like coupling constant, mass, etc) appear to vary on differing length or energy scales. To see how this works for the strong coupling constant, we note that α_s is

$$\alpha_s\left(Q^2\right) = \frac{4\pi}{(11 - 2n_f/3)\ln\left(Q^2/\Lambda^2\right)}, \tag{1.8}$$

where Λ is the QCD scale fixed by various scattering processes and is currently believed to range from 100 MeV to 300 MeV, and n_f is the number of flavors. Since $n_f = 6$, the coupling constant decreases with increasing momentum transfer Q^2. So at very large energy scales corresponding to very high momentum transfer the coupling constant becomes vanishingly small rendering the theory asymptotically free. This is the domain of asymptotic freedom of QCD [4]; asymptotic freedom allows us to treat quarks and gluons as essentially free at very high energies, leading to Bjorken scaling, and permits us to use perturbative QCD in this regime. On the other hand, at low energies or large distance scales the coupling constant is large making the interaction among quarks and gluons strong and a perturbative treatment, based on an expansion in powers of α_s, is untenable. This, therefore, calls for a non-perturbative treatment.

Thus, if we have a collection of quarks and gluons at a temperature much higher than several hundred MeV, then they will interact among themselves with momentum transfer much higher than Λ, which has a typical value, as revealed by scattering experiments, of about 200 MeV. Asymptotic freedom will then ensure that α_s be small such that the quarks and gluons are no more constrained to remain confined to regions typically of the size of a hadron ($\sim$ 1 fm) and behave, instead, like a weakly interacting, almost ideal gas-like, system of quarks and gluons - the so-called quark-gluon plasma (QGP). Another possibility is that if we have baryonic matter compressed to very high densities such as that believed to exist in the cores of neutron stars, the hadrons almost overlap and the separation between the constituent quarks and gluons typically becomes of the order of 1 fm or $(200MeV)^{-1}$ making, as before,

α_s very small, making it possible for matter to exist, once again, in a QGP-like state. However, should temperatures be not very high, many body quantum effects are likely to play a dominant role and it is speculated that under such conditions matter could even exist in such exotic states as the color superconductor or the color superfluid.

1.3 QCD at finite temperature

A systematic study of QGP as a weakly interacting system of quarks and gluons at high temperatures demands a statistical description of quantum fields. In this section we first make a digression to say a few words about the basic formalism of finite temperature field theory and then come back to a very specific discussion of a system of fermions (quarks) and bosons (gluons) at a finite temperature.

1.3.1 The Partition Function

It is well known from statistical mechanics that the partition function

$$\begin{aligned} Z &= \text{Tr } e^{-\beta H} \qquad \text{where } \beta = \frac{1}{T} \\ &= \int d\phi_a \, \langle \phi_a \mid e^{-\beta H} \mid \phi_a \rangle, \end{aligned} \tag{1.9}$$

with Tr denoting the trace or the sum over the expectation values in any complete basis, encapsulates all possible information about the thermal properties of a system in equilibrium. Now, in path integral formalism the expression for transition amplitude is

$$\begin{aligned} \langle \phi_1 \mid e^{-i\,H(t_1-t_2)} \mid \phi_2 \rangle &\simeq \langle \phi(\vec{x_1}, t_1) \mid \phi(\vec{x_2}, t_2) \rangle \\ &= N \int D\phi \, e^{iS} \end{aligned} \tag{1.10}$$

where N is a normalization constant, ϕ, the basic quantum field variable, and S is the action.

$$S[\phi] = \int_{t_2}^{t_1} dt \int d^3x \, L \tag{1.11}$$

where L is the Lagrangian density. The path integral is performed over paths satisfying

$$\phi(\vec{x_1}, t_1) = \phi_1, \quad \text{and} \quad \phi(\vec{x_2}, t_2) = \phi_2, \tag{1.12}$$

with ϕ_1, ϕ_2 as the fixed end points which do not come under the scope of the integration operation.

A comparison of equations (9) and (10) show that with the identification of $t_1 - t_2$ with $-i\beta$, Z can be cast in the form of a path integral.Thus

$$\begin{aligned} Z(\beta) &= \text{Tr } e^{-\beta H} = \int d\phi_1 \, \langle \phi_1 \mid e^{-\beta H} \mid \phi_1 \rangle \\ &= N \int D\phi \, e^{-S_E} \end{aligned} \tag{1.13}$$

where S_E is the Euclidean action ($t \to i\,t$),

$$S_E = \int_0^\beta d\tau \int d^3x \, L_E. \tag{1.14}$$

The following points are in order in this context. First, since we are interested in evaluating a trace, we require that in the path integral the integration be performed only over those field variables which satisfy periodic boundary conditions

$$\phi(\vec{x}, \beta) = \phi(\vec{x}, 0). \tag{1.15}$$

Second, as Tr $e^{-\beta H}$ involves a sum over states, here the end points too need to be integrated over.
Now, thermal Green's function, defined by

$$G(x, y; \tau, 0) = Z^{-1} \, \text{Tr} \, (e^{-\beta H} \, T[\phi(x, \tau) \, \phi(y, 0)]) \tag{1.16}$$

where T is the imaginary time ordering operator, provides information on the boundary conditions on the field variables. For bosons we have

$$T[\phi(\tau_1) \, \phi(\tau_2)] = \phi(\tau_1) \, \phi(\tau_2) \, \theta(\tau_1 - \tau_2) + \phi(\tau_2) \, \phi(\tau_1) \, \theta(\tau_2 - \tau_1), \tag{1.17}$$

whereas for fermions, in view of their anticommuting properties, we have

$$T[\psi(\tau_1) \, \psi(\tau_2)] = \psi(\tau_1) \, \psi(\tau_2) \, \theta(\tau_1 - \tau_2) - \psi(\tau_2) \, \psi(\tau_1) \, \theta(\tau_2 - \tau_1). \tag{1.18}$$

It follows from the above that for bosons

$$\begin{aligned} G(x, y; \tau, 0) &= G(x, y; \tau, \beta) \quad \text{and} \\ \phi(y, 0) &= \phi(y, \beta), \end{aligned} \tag{1.19}$$

and for fermions

$$\begin{aligned} G(x, y; \tau, 0) &= -\, G(x, y; \tau, \beta) \quad \text{and} \\ \psi(x, 0) &= -\, \psi(x, \beta). \end{aligned} \tag{1.20}$$

This implies that in the path integral representation of the partition function, the integration over the field variables is restricted only to those fields which, for the bosons, are periodic in imaginary time with a period β and, for the fermions, are

antiperiodic in imaginary time with a period β.

We have given, in bare outline, the way to construct the partition function for a QCD system [6]. Armed with the partition function we can, in principle, evaluate all thermodynamic variables of relevance. However, as a next exercise, we choose an alternative route to evaluate expressions for pressure and energy density of a relativistic system of weakly interacting fermions [7]. To begin with, we consider quarks first.

1.3.2 Quarks :

The Fermi-Dirac distribution gives us the number of quarks in a volume V, temperature T, and with momentum between p and $p + dp$ as

$$dN_q = g_q\, V\, \frac{4\pi p^2 dp}{(2\pi)^3}\, \frac{1}{1 + e^{(p-\mu_q)/T}}, \tag{1.21}$$

where μ_q is the quark Fermi energy or chemical potential, and $g_q = N_c N_s N_f$ is the number of independent degrees of freedom of quarks or quark degeneracy. When the number density of quarks is the same as that of antiquarks, $\mu_q = 0$. Hence the energy of massless quarks ($E \simeq p$) is given by

$$E_q = \frac{g_q V}{2\pi^2} \int_0^\infty \frac{p^3\, dp}{1 + e^{p/T}}. \tag{1.22}$$

The above integration can be performed by invoking the Γ function and the Riemann zeta function. This yields

$$E_q = \frac{7}{8}\, g_q\, V \frac{\pi^2}{30}\, T^4. \tag{1.23}$$

It is known from statistical mechanics that for massless fermions and bosons the pressure P is related to the energy density $\rho = E/V$ as

$$P = \frac{1}{3}\, \rho\,. \tag{1.24}$$

Thus, the pressure due to quarks is

$$P_q = \frac{7}{8}\, g_q\, \frac{\pi^2}{90}\, T^4, \tag{1.25}$$

and that due to antiquarks is given by the same expression with g_q replaced by $g_{\bar{q}}$. Hence the total pressure exerted by quarks and antiquarks present in the system is

$$P_q \,+\, P_{\bar{q}} = \frac{7}{8}\, (\, g_q \,+\, g_{\bar{q}})\, \frac{\pi^2}{90}\, T^4. \tag{1.26}$$

And the number density of quarks and antiquarks is

$$\begin{aligned} n_q &= n_{\bar{q}} = \frac{g_q}{2\pi^2} \int_0^\infty \frac{p^2\, dp}{1 + e^{p/T}} \\ &= \frac{g_q}{2\pi^2}\, T^3\, \frac{3}{2}\, \zeta(3)\,, \end{aligned} \tag{1.27}$$

where $\zeta(3) = 1.20206$.

1.3.3 Gluons :

We now repeat the above procedure for a weakly interacting system of gluons occupying a volume V and at temperature T. The energy of the system is

$$E_g = \frac{g_g V}{2\pi^2} \int_0^\infty p^3\, dp \left\{ \frac{1}{e^{p/T} - 1} \right\}, \tag{1.28}$$

where the bracketed term is the Bose-Einstein distribution for bosons and g_q is the gluon degeneracy,

$$g_g = (\text{number of different gluons}, 8) \times (\text{number of polarizations}, 2) = 16. \tag{1.29}$$

On integrating the above the way it was done in the case of quarks, we get

$$E_g = g_g\, V \frac{\pi^2}{30}\, T^4. \tag{1.30}$$

Again, using $P = \frac{1}{3}\, \rho$, we get the pressure for the gluon gas as

$$P_g = g_g\, \frac{\pi^2}{90}\, T^4. \tag{1.31}$$

We notice that the expressions for E_g and P_g are exactly the same as those for quarks save for the absence of the factor $\frac{7}{8}$.

The number density of gluons is

$$\begin{aligned} n_g &= \frac{g_g}{2\pi^2} \int_0^\infty \frac{p^2\, dp}{e^{p/T} - 1} \\ &= \frac{g_g}{2\pi^2}\, T^3\, \Gamma(3)\, \zeta(3) = 1.20206\, \frac{g_g}{\pi^2}\, T^3. \end{aligned} \tag{1.32}$$

We are finally in a position to write down the net energy density of a system of quarks and gluons at temperature T:

$$\begin{aligned} \rho_{QGP} &= \rho_{q\bar{q}} + \rho_g \\ &= \left[\frac{7}{8}\, (g_q + g_{\bar{q}}) + g_g \right] \frac{\pi^2}{30}\, T^4 \\ g_q &= g_{\bar{q}} = N_C\, N_S\, N_F = 3 \times 2 \times 6. \end{aligned} \tag{1.33}$$

Here N_C, N_S, and N_F are the number of color, spin, and flavor states of quarks and $g_g = 16$, so

$$\rho_{QGP} = \left(\frac{7}{8} \times 72 + 16\right) \frac{\pi^2}{30} T^4 \tag{1.34}$$

The implicit assumption in all this is that the temperature of the system is such that all the quark flavors can be treated as being massless, an assumption valid only for $T \gg m_{top} \simeq 170\, GeV$.

To develop a feel for the situation let us calculate ρ_{QGP} at the expected transition temperature of $T = 200$ MeV. At this temperature we can take only u and d quarks to be approximately massless so that

$$g_{q+\bar{q}} = 2 \times 3 \times 2 \times 2 = 24, \tag{1.35}$$

where N_C, N_S, N_F, q, and $\bar{q}$ all correspond to u and d quarks only. Hence

$$\begin{aligned} \rho_{QGP} &= \left(\frac{7}{8} \times 24 + 16\right) \frac{\pi^2}{30} T^4 \\ &= \frac{37\pi^2}{30} T^4. \end{aligned} \tag{1.36}$$

Further, for $T = 200\,\text{MeV}$ and using $1\,\text{fm} = (200\,\text{MeV})^{-1}$, we get $\rho_{QGP} \simeq \frac{37}{3}\,(200\,\text{MeV})^4 \simeq 2.5\,\text{GeV/fm}^3$. We conclude, therefore, that should we be able to create a dense system of partons (quarks and gluons) with an energy density greater than the above estimate and, if we can further make a case for thermal equilibrium for such a system, then we can claim with a certain degree of confidence that a state of QGP will be achieved. Such a scenario is expected to be realized in relativistic heavy-ion collision experiments where the nuclei impacting at ultra high energies create a soup of quarks, antiquarks and gluons with a central energy density most likely to be well above 3 GeV/fm^3.

1.4 Quark Confinement

As we have already mentioned, a huge body of experimental work seems to indicate that quarks and gluons do not exist free in nature and there is confinement of quarks and gluons in a hadron so that only color singlets can be produced and observed.This fact that no naturally occurring particles carry color is known as color confinement. In particular, quarks are packaged in colorless packages of two (mesons) and three (baryons). Self-coupling of gluons allows the possibility of the existence of colorless bound states of gluons, known as glueballs, although none has been detected so far yet. If QCD is to claim itself as the correct theory of quarks and gluons it must contain the explanation for quark confinement. Although the notion finds support from hadron spectroscopy and lattice QCD results, no rigorous theoretical basis for

quark confinement is available. The problem springs from the fact that color confinement involves the long-range behavior of quark-quark interaction and this is precisely the regime in which perturbative QCD fails. It is surmised that the force operating between quarks has a Coulomb-like part and a confining part, which increases with distance and makes it impossible to isolate quarks. The confining part owes its origin to multi gluon exchange between quarks. This, however, is a conjecture only begging for a conclusive proof.

1.4.1 The MIT Bag Model

A phenomenological model which incorporates both asymptotic freedom and color confinement is the MIT bag model [8], which is one among many different versions of the Bag model. In this model a colorless hadron exists as a spherical bag of radius R, where R is less than 1 fm to ensure smallness of the coupling constant, and colored quarks and gluons stay confined in this bag as almost free entities. Thus the bag incorporates the physics of confinement while the freedom of the constituents inside reflect the spirit of asymptotic freedom. The quarks are treated as massless particles inside the bag and and are infinitely massive outside, in tune with the coupling constant becoming large at large distances. The kinetic energy of the quarks gives rise to an internal pressure trying to inflate the bag which is counteracted by an external bag pressure B trying to achieve the very opposite i.e. deflate the bag. A balance of these two pressures serves to stabilize the hadron. The phenomenological quantity B is introduced to take into account the non-perturbative color confining effects of QCD. The model can accommodate glueballs too by allowing gluonic fields confined inside the bag.

With such a simple model for a hadron we next try to estimate the bag pressure by considering massless free fermions trapped inside a spherical cavity of radius R. The Dirac equation for a free massless fermion in the cavity is

$$\gamma.p\,\psi = 0. \tag{1.37}$$

We recall that the Dirac representation of the γ matrices are

$$\gamma^0 = \begin{pmatrix} I & 0 \\ 0 & -I \end{pmatrix} \tag{1.38}$$

and

$$\gamma^i = \begin{pmatrix} 0 & \sigma^i \\ -\sigma^i & 0 \end{pmatrix}, \tag{1.39}$$

Where I is a 2×2 unit matrix and σ^i are the Pauli matrices. We express the four

component wave function ψ for the massless fermions as

$$\psi = \begin{pmatrix} \psi_+ \\ \psi_- \end{pmatrix}, \tag{1.40}$$

where ψ_+ and ψ_- are two dimensional Dirac spinors. Plugging the above into eq. (37) we get

$$\begin{pmatrix} p_0 & -\vec{\sigma}.\vec{p} \\ +\vec{\sigma}.\vec{p} & -p_0 \end{pmatrix} \begin{pmatrix} \psi_+ \\ \psi_- \end{pmatrix} = 0 \tag{1.41}$$

On solving the above equation one gets the ground state solution as

$$\psi(\vec{r},t) = \begin{pmatrix} \psi_+(\vec{r},t) \\ \psi_-(\vec{r},t) \end{pmatrix} = \begin{pmatrix} A\, e^{-ip_0 t}\, j_0\left(p^0 r\right) \chi_+ \\ A\, e^{-ip_0 t}\, (\vec{\sigma}.\vec{r})\, j_1\left(p^0 r\right) \chi_+ \end{pmatrix}$$

where j_0 & j_1 are spherical Bessel functions, $\chi_\pm$ are Dirac spinors, and A is a normalization constant.

Now, for quarks to remain confined to the bag , the normal component of the vector current $j^\mu = \bar{\psi}\gamma^\mu\psi$ must vanish at the surface or, equivalently, the scalar density $\bar{\psi}\,\psi$ vanishes at the bag surface at R. This leads to

$$j_0(p^0 R) = j_1(p^0 R) \tag{1.42}$$

This has a solution

$$p^0 R = 2.04 \quad \text{or,} \quad \mathrm{p}^0 = \frac{2.04}{\mathrm{R}}. \tag{1.43}$$

It is easy to show from the uncertainty principle that the kinetic energy of a quark inside a bag is inversely proportional to the radius of the bag. The total energy of a system of N quarks confined to a bag of radius R is

$$E = \frac{2.04N}{R} + \frac{4}{3}\pi R^3 B, \tag{1.44}$$

where the last term originates from the bag pressure. By minimizing the total energy we get the equilibrium radius as

$$B^{\frac{1}{4}} = \left(\frac{2.04N}{4\pi}\right)^{\frac{1}{4}} \frac{1}{R}. \tag{1.45}$$

If we take 0.8 fm to be the confinement radius for a baryon, then we get the following estimate for B

$$B^{\frac{1}{4}} = 206\mathrm{MeV}. \tag{1.46}$$

The value of $B^{\frac{1}{4}}$ is, however, model-specific and ranges from 145 MeV to 235 MeV. For a more detailed treatment see [9].

1.4.2 Transition to the QGP state in the Bag Model

The physics of the bag model, simply put, is - the bag holds only as long as the pressure within equals the inward bag pressure and, in the event that the pressure inside exceeds the inward bag pressure, the bag yields, setting free the heretofore confined quarks and gluons. We then have a new phase of matter containing quarks and gluons and the liberated quarks and gluons soon reach a state of thermal equilibrium. The phase is known as the deconfined phase of partonic mater or the Quark-Gluon Plasma.

The factor crucial to the creation of a QGP phase is a large inner pressure exceeding the bag pressure which can come about in two ways :

1. When the temperature of the system is high, as what happened in the early universe.

2. when the baryon density is high, as in the cores of neutron stars.

Let us now explore the two possibilities.

1.4.3 Quark Gluon Plasma at High Temperature

We recall that the total pressure of a quark-gluon system at temperature T and zero baryon density is

$$\begin{aligned} P &= g_{total}\,\frac{\pi^2}{90}\,T^4 \\ g_{total} &= \left[\frac{7}{8}\,(g_q + g_{\bar{q}}) + g_g\right]. \end{aligned} \tag{1.47}$$

By considering only u and d quarks we have calculated g_{total} to be 37. Hence

$$P = \frac{37\pi^2}{90}\,T^4. \tag{1.48}$$

We equate it to the bag pressure B to estimate the critical temperature for transition to QGP state

$$\begin{aligned} \frac{37\pi^2}{90}\,T_c^4 &= B \\ \Rightarrow T_c &= \left[\frac{90B}{37\pi^2}\right]^{\frac{1}{4}} \end{aligned} \tag{1.49}$$

With the value of $B^{\frac{1}{4}} = 206\ MeV$ as estimated in the previous section, we get $T_c \sim 144\ MeV$. Current estimates of T_c obtained from lattice calculations puts it at about 154 MeV [14].

1.4.4 Quark Gluon Plasma at High Baryon Density

We now examine the possibility of a deconfining pressure developing inside a bag even at $T = 0$ due to high baryon density. Pressure in such a situation arises from the

Fermi momentum of quarks and because of high baryon number density we can safely ignore the effect of antiquarks and gluons. The number of states in a volume V and within a momentum interval dp about p is

$$\frac{g_q\,V}{(2\pi)^3}\,4\pi p^2 dp. \tag{1.50}$$

Since because of Pauli's exclusion principle no more than one quark can populate each state, the total number of quarks, up to the quark Fermi momentum μ_q (i.e. the chemical potential) is

$$\begin{aligned} N_q &= \frac{g_q\,V}{(2\pi)^3}\int_0^{\mu_q} 4\pi p^2 dp \\ &= \frac{g_q\,V}{6\pi^2}\,\mu_q^3. \end{aligned} \tag{1.51}$$

The number density of quarks, therefore, is

$$n_q = \frac{g_q}{6\pi^2}\,\mu_q^3. \tag{1.52}$$

The energy of the quark gas in a volume V is

$$\begin{aligned} E_q &= \frac{g_q\,V}{(2\pi)^3}\int_0^{\mu_q} 4\pi p^3 dp \\ &= \frac{g_q\,V}{8\pi^2}\,\mu_q^4. \end{aligned} \tag{1.53}$$

Therefore the energy density is

$$\rho_q = \frac{g_q}{8\pi^2}\,\mu_q^4. \tag{1.54}$$

Again, from the relation between the pressure and the energy density, we have

$$P_q = \frac{1}{3}\,\rho = \frac{g_q}{24\pi^2}\,\mu_q^4. \tag{1.55}$$

Quark matter inside the bag will undergo a transition to the QGP state for a critical value of $\mu_q \simeq \mu_c$ when $P_q = B$. Thus

$$P_q = B = \frac{g_q}{24\pi^2}\,\mu_c^4, \tag{1.56}$$

leading to

$$\mu_c = \left[\frac{24\,\pi^2 B}{g_q}\right]^{\frac{1}{4}}. \tag{1.57}$$

Substituting this in equation (52), we get a critical number density of quarks as

$$n_q^{critical} = 4\,\left(\frac{g_q}{24\,\pi^2}\right)^{\frac{1}{4}}\,B^{\frac{3}{4}}. \tag{1.58}$$

The corresponding critical baryon density is

$$n_B^{critical} = \frac{4}{3}\left(\frac{g_q}{24\,\pi^2}\right)^{\frac{1}{4}} B^{\frac{3}{4}}. \tag{1.59}$$

Considering only the flavors u and d, $g_q = 3 \times 2 \times 2 = 12$ for 3 colors, 2 spins and 2 flavors.
Using $B^{\frac{1}{4}} = 206\ MeV$ we get $\mu_c = 434\ MeV$ and the corresponding critical baryon number density is $n_c = 0.72/fm^3$. In contrast, the nucleon number density in normal nuclear matter in equilibrium is $n_B = 0.16/fm^3$. So the critical baryon density is about 5 times the normal nuclear matter density. When the density of baryons exceeds the critical density, the pressure due to the degenerate quark matter inside the bag gets the better of the baryon bag pressure leading to a new deconfined QGP state. And, for a system at finite temperature and having a finite chemical potential, the critical values for temperature and baryon chemical potential will lie somewhere in between the values for the two extreme cases we have discussed.

The QCD phase diagram encapsulates our current understanding of different phases of QCD matter. The QCD phase diagram as a function of temperature (T) and baryon chemical potential μ_B is shown in Fig.1.1 [10]. The diagram furnishes information on different phases of QCD and associated phase transitions. The qualitative aspects of this phase diagram is best studied if one divides the diagram into three different regions.

A lot of results are available from lattice simulation for the region with zero chemical potential and high temperatures. Lattice calculations based on realistic values of quark masses predict that there are no genuine phase transitions for $\mu_B = 0$. This rules out the existence of any phase boundary in this direction. Calculations point toward a crossover from the hadronic phase to the quark-gluon plasma phase for realistic u, d and s quark masses [11,12]. The crossover temperature is likely to be in the range $150 - 200\ MeV$. Such temperatures prevailed in the early universe and experiments like RHIC and LHC have targeted this region to explore phase transitions for very small μ_B.

Now moving along the μ_B direction at zero temperature we are confronted with a rich possibility of phase structures. First to make appearance is nuclear matter for $\mu_B \sim 940\,MeV$, separated from the hadronic gas by a first order transition line. Continuing beyond up to larger values of μ_B one expects to find neutron superfluidity, as within neutron star cores, where neutrons condense to form a superfluid. At still higher values of μ_B high density QGP is expected to form. Several exotic phase are possible too, like - color superconductor, resulting from the condensation of quark Cooper pairs (as in normal superconductors where we have electron-electron Cooper pairs). Properties of such phases are not very well-understood. For a review see ref. [13]. Other exotic phases proposed are [10] the Color Flavor Locked (CFL) phase and the crystalline color superconductor phase. The core of neutron star is likely to contain all these phases. The proposed experiment on compressed baryonic

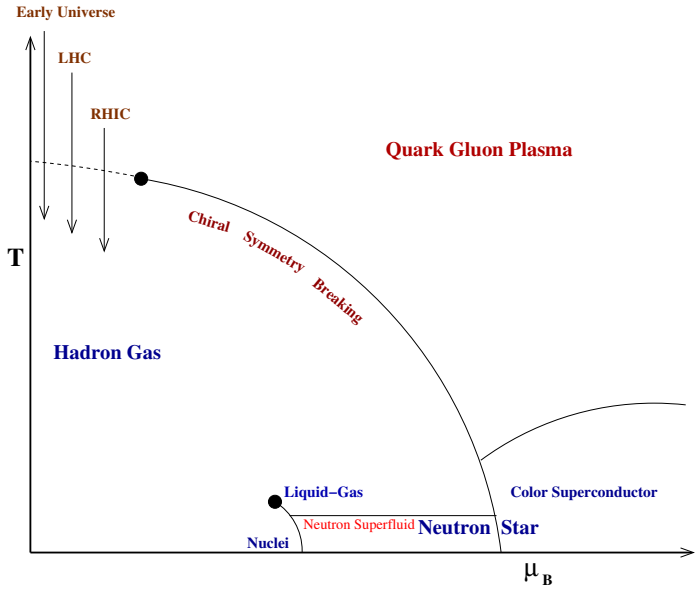

Figure 1.1: QCD phase diagram (see ref. [10]).

matter (CBM) at FAIR is expected to throw some light on this high μ_B region of QCD.

For finite T and finite μ_B there are very few lattice calculations available. In this region effective field theory models predict first order phase transition. Combining this with lattice results which predict a crossover for small μ_B, we conclude that the first order transition line should end with $T = T_c$ and $\mu_B = \mu_c$ at which the phase transition is second order. This point is the critical point in the phase diagram. Several experiments aim to explore this critical point.

The QCD phase diagram is a treasuretrove of many open questions begging for an answer. Several experiments are going on and several more are planned to find answers to these questions.

With that we come to the end of our brief introduction to QCD. The rest of the thesis is organized as follows:

Chapter 2 discusses some of the concepts which bear upon our own work, like - QCD phase transitions, DCC formation, a general discussion of phase transitions highlighting some of its key concepts, and concludes with a short note on heavy ion collisions and QGP signatures.

Chapter 3 continues in the spirit of its predecessor and introduces another key ingredient of our work - the reaction diffusion equation. The equation is developed in the backdrop of the diffusion equation. We mention some popular incarnations of it and show how travelling wave solutions arise in the asymptotic limit.

Chapters 4 and 5 describe our own work. In chapter 4 we show how some specific versions of the reaction-diffusion equation, with appropriate boundary conditions, govern the dynamics of the order parameter for both chiral symmetry breaking transition and confinement-deconfinement transition, with dissipative dynamics, in heavy-ion collisions. We show that the transitions are completed by a propagating interface.

In Chapter 5 we discuss the possibility of DCC formation in high multiplicity pp collisions at LHC energy by applying the reaction-diffusion equation to the dynamics of the chiral field after the symmetry breaking transition. We argue that a single large domain of DCC is a possibility within the interior of a rapidly expanding quark-gluon plasma.

In Chapter 6 we summarize our results.

Bibliography

[1] F.Halzen, A.D Martin, *Quarks And Leptons* (John Wiley and Sons); D.Griffiths, *Introduction to Elementary Particles* (John Wiley and Sons), 1987; D.H.Perkins, *Introduction to High Energy Physics* (Addison-Wesley Publishing Company), 1982; Fayyazuddin, Riazuddin, *A Modern Introduction to Particle Physics* (World Scientific, Singapore), 2000.

[2] J. D. Bjorken, Phys. Rev. **179**, 1547 (1969).

[3] R. P. Feynman, Phys. Rev. Lett. **23**, 1415 (1969).

[4] D. J. Gross and F. Wilczek, Phys. Rev. Lett. **30**, 1343 (1973); H. D. Politzer, Phys. Rev. Lett. **30**, 1346 (1973).

[5] M. E. Peskin and D. V. Schroeder, *An Introduction to Quantum Field Theory*, (Addison Wesley, Reading, USA), 1995; L. H. Ryder, *Quantum Field Theory*, (Cambridge University Press, Cambridge, UK), 1985; T. Cheng and L. Li, *Gauge Theory Of Elementary Particles*, (Oxford University Press), 2005; R. Rangarajan and M. Sivakumar (Ed), *Surveys in Theoretical High Energy Physics 2*, (Hindusthan Book Agency), 2014.

[6] J. I. Kapusta, *Finite Temperature Field Theory*, (Cambridge University Press, Cambridge, UK), 1989; A. Das, *Finite Temperature Field Theory*, (World Scientific, Singapore), 1997.

[7] C. Y. Wong, *Introduction to High-Energy Heavy Ion Collisions*, (World Scientific, Singapore), 1994.

[8] A. Chodos, R. L. Jaffe, K. Johnson, C. B. Thorn, and V. F. Weisskopf, Phys. Rev. D**9**, 3471 (1974); T. Degrand, R. L. Jaffe, K. Johnson, and J. E. Kiskis, Phys. Rev. D**12**, 2060 (1975).

[9] F. E. Close, *Introduction to Quarks and Partons*, (Academic Press, London), 1979.

[10] K. Fukushima and T. Hatsuda, Rept. Prog. Phys. **74**, 014001 (20110 [arXiv:1005.4814[hep-ph]]

[11] Y. Aoki, G. Endrodi, Z. Fodor, S. D. Katz, and K. K. Szabo, Nature, **443**, 675 (2006) [hep-lat/0611014].

[12] C. DeTar and U. M. Feller, Eur. Phys. J. A, **41**, 405 (2009) [hep-lat:0905.2949].

[13] K. Rajagopal and F.Wilczek, in Shifman, M. (ed.) : At the Frontier of Particle Physics, vol. 3, 2061-2151 [hep-ph/0011333].

[14] H. T. Ding, F. Karsch and S. Mukherjee, "Thermodynamics of strong-interaction matter from Lattice QCD," Int. J. Mod. Phys. E **24**, no. 10, 1530007 (2015)

Chapter 2

QCD Phase Transitions

The purpose of this chapter is to discuss QCD phase transitions. Our first topic of discussion will be confinement-deconfinement transition (section 2.1) and we shall follow it up in section 2.2 with a discussion of chiral transition. This will lead us to DCC in section 2.3. Finally, in sections 2.4 and 2.5 we shall have a few words to say about first and second order transitions and relativistic heavy-ion collisions, pertinent, as they are, to our work embodied in chapters four and five.

2.1 Confinement Deconfinement Phase Transition

In this section we follow [1] to construct the order parameter for the phase transition and then write the effective potential for the order parameter. We shall work with pure QCD with no dynamical quarks in the picture.

2.1.1 Polyakov Loop Order Parameter

Consider $SU(N)$ gauge theory at finite temperature without dynamical quarks. Let $|s_G\rangle$ denote the states of the system. The partition function of the system is

$$\mathcal{Z} = e^{-\beta F} = \sum_{s_G} \langle s_G | e^{-\beta H} | s_G \rangle. \tag{2.1}$$

As we know, the phases of a nonabelian gauge theory (with the possibility of a confining phase) can be characterized by the free energy of a static configuration of quarks and antiquarks. We introduce operators, $\psi_a^\dagger(\vec{x_0}, t)$ and $\psi_a(\vec{x_0}, t)$ which create and annihilate static quarks with color a at position $\vec{x_0}$, and time t, along with their charge conjugates for antiquarks. These operator fields satisfy the anticommutation relations

$$\{\psi_a(\vec{x_1}, t), \psi_b^\dagger(\vec{x_2}, t)\} = \delta_{ab}\delta^3(\vec{x_1} - \vec{x_2}). \tag{2.2}$$

Conjugates enjoy a similar relation and all other equal-time anticommutators vanish.

Now, the Dirac equation in Euclidean space gives the (Euclidean) time evolution of the wave function. Thus

$$\left(-i\partial_0\delta^{ab} - gA_0^{ab}(\vec{x_0},\tau)\right)\psi_b(\vec{x_0},\tau) = 0, \tag{2.3}$$

where $A_0 = A_0^i\lambda_i$, with λ_i being the Gell-Mann matrices. This gives the solution as

$$\psi_a(\vec{x_0},\beta) = \mathbf{P}\left[\exp\left(ig\int_0^{\tau=\beta} d\tau A_0(\vec{x_0},\tau)\right)\right]_{ab}\psi_b(\vec{x_0},0), \tag{2.4}$$

where $\mathbf{P}$ denotes path ordering forward in time.

Now in order to determine whether the system is in confined or deconfined phase, we probe the system with an infinitely heavy test quark, placed at the position $\vec{x_0}$. To eliminate the possibility of any back reaction of the test quark on the system the probe is kept static which is possible only if the test quark is infinitely heavy.The presence of the test quark alters the state of the system to $|s\rangle = \psi_a^\dagger(\vec{x_0},0)|s_G\rangle$. Hence the partition function is

$$\begin{aligned}\mathcal{Z}_q = e^{-\beta F(\vec{x_0})} &= \frac{1}{N}\sum_s \langle s|e^{-\beta H}|s\rangle, \\ &= \frac{1}{N}\sum_{s_G}\langle s_G|\sum_a \psi_a(\vec{x_0},0)e^{-\beta H}\psi_a^\dagger(\vec{x_0},0)|s_G\rangle,\end{aligned} \tag{2.5}$$

where N is the number of colors. It is three for QCD. Thus the sum over a is on all the possible color states. Here the sum is over all states $|s_G\rangle$ with no quarks, that is, over states of pure glue theory. Now time translation in Euclidean space is generated by $e^{-\beta H}$ in much the same way as the operator e^{-iHt} generates time translation in Minkowski time. Thus, in Euclidean space, for any operator O,

$$e^{\beta H}O(t)e^{-\beta H} = O(t+\beta), \tag{2.6}$$

which implies

$$e^{\beta H}\psi_a(\vec{x_0},0)e^{-\beta H} = \psi_a(\vec{x_0},\beta), \tag{2.7}$$

$$\Rightarrow \mathcal{Z}_q = \frac{1}{N}\sum_{s_G}\langle s_G|\sum_a e^{-\beta H}\psi_a(\vec{x_0},\beta)\psi_a^\dagger(\vec{x_0},0)|s_G\rangle. \tag{2.8}$$

The time evolved field in Eq.(2.4) and the initial field are related by an overall phase which is the non-abelian analogue of Bohm-Aharonov phase and is called the Wilson line. It is, however, a loop in the Euclidean space due to the periodicity in time direction. The trace of this quantity over all color degree of freedom is known as Polyakov Loop. It is defined as

$$L(\vec{x}) = \frac{1}{N}\mathrm{Tr}\left\{\mathbf{P}\left[\exp\left(ig\int_0^{\tau=\beta} d\tau A_0(\vec{x_0},\tau)\right)\right]\right\}. \tag{2.9}$$

Using eq. (2.4) and eq. (2.9) in eq. (2.8) we get

$$\mathcal{Z}_q = \sum_{s_G} \langle s_G | e^{-\beta H} L(\vec{x}) | s_G \rangle. \tag{2.10}$$

If we divide the above equation by the partition function of the pure glue system, we get the change in the free energy of the system due to the introduction of the infinitely heavy quark

$$\frac{\mathcal{Z}_q}{\mathcal{Z}} \equiv e^{-\beta \Delta F} = \langle L(\vec{x}) \rangle. \tag{2.11}$$

Since our test quark is static and infinitely massive it does not make much sense to talk about its free energy. However, with a quark and an antiquark pair at positions $\vec{x}$ and $\vec{y}$ respectively, one can show that the free energy of the system is a function of the distance between the pair. Thus

$$\langle L^\dagger(\vec{y}) L(\vec{x}) \rangle \propto e^{-\beta F_{q\bar{q}}}. \tag{2.12}$$

- **For confining phase**, the free energy required to separate a quark- antiquark pair is infinite. That means $F_{q\bar{q}} \to \infty$ as the separation between the pair increases. Also, for a very large distance between the pair one expects their Polyakov loops to be uncorrelated. Thus $\langle L^\dagger(\vec{y}) L(\vec{x}) \rangle \longrightarrow \langle L^\dagger(\vec{y}) \rangle \langle L(\vec{x}) \rangle = |\langle L(\vec{x}) \rangle|^2$. Then Eq.(2.12) becomes

  $$|\langle L(\vec{x}) \rangle|^2 \propto e^{-\beta F_{q\bar{q}}}. \tag{2.13}$$

  Hence $\langle L(x) \rangle = 0$ in the confining phase.

- **For deconfined phase**, $F_{q\bar{q}}$ is finite, hence $\langle L(x) \rangle$ is finite. One can normalize $\langle L(x) \rangle$ to unity.

Thus the Polyakov loop can serve as an order parameter to distinguish the confined phase from the deconfined phase. It vanishes in the confined phase and becomes unity in the deconfined phase at high temperature.

2.1.2 Effective potential for Order Parameter

In this section we make the following notational changes - we suppress the arrow on $\vec{x}$ and denote the thermal expectation of the Polyakov loop by the symbol $l(x)$. We work with the effective Lagrangian of the Polyakov loop as proposed by Pisarski [2,3]

$$\mathcal{L} = \frac{N}{g^2} |\partial_\mu l|^2 T^2 - V(l), \tag{2.14}$$

where

$$V(l) = \left(-b_2 |l|^2 + b_3 (l^3 + (l^*)^3) + |l|^4 \right) b_4 T^4. \tag{2.15}$$

l being dimensionless, the factor T^4 determines the dimensions of the potential. In mean field theory, b_4 is taken as constant and b_2 varies with temperature. For $b_3 \neq 0$, the Lagrangian has $Z(3)$ symmetry. The parameters are fitted in ref. [4–6] such that that the effective potential reproduces the thermodynamics of pure $SU(3)$ gauge theory on lattice [7, 8]. The coefficients are $b_2 = (1 - 1.11/x)(1 + 0.265/x)^2 (1 + 0.300/x)^3 - 0.478$, (with $x = T/T_c$ and $T_c \sim 182$ MeV), $b_3 = 2.0$ and $b_4 = 0.6061 \times 47.5/16$. With these values, $l(x) \longrightarrow y = b_3/2 + \frac{1}{2} \times \sqrt{b_3^2 + 4b_2\,(T = \infty)}$ as $T \longrightarrow \infty$. Various quantities are then rescaled such that $l(x) \longrightarrow 1$ as $T \longrightarrow \infty$. The scalings are

$$l(x) \to \frac{l(x)}{y}, \quad b_2 \to \frac{b_2}{y^2}, \quad b_3 \to \frac{b_3}{y}, \quad b_4 \to b_4 y^4. \tag{2.16}$$

l has the value zero at low temperatures and the potential has only one minimum. For $T > T_c$, $l(x)$ picks up a nonvanishing vacuum expectation value l_0, and the cubic piece above spawns three degenerate vacua, known as $Z(3)$ vacua. The structure of these $Z(3)$ vacua has been discussed in the literature. Our work will not refer to this $Z(3)$ structure, hence we shall not discuss this here.

2.2 Chiral Symmetry Breaking

Apart from the $SU(3)$ color gauge symmetry, which is exact, QCD possesses two approximate global symmetries - namely, isospin symmetry, and chiral symmetry, with associated transition known as chiral phase transition [9]. While the isospin flavor symmetry played a decisive role in the early days of QCD and was instrumental in the genesis of the quark model, the chiral symmetry is a very important symmetry of QCD which arises in the vanishing mass limit of certain quark flavors, in particular the u and the d quarks whose masses are small compared to the QCD scale, leading to decoupling of the left and the right handed components of the massless quarks.

To appreciate the realization of chiral symmetry breaking in QCD and the consequent appearance of pions as Goldstone bosons, let us start with the QCD Lagrangian

$$\mathcal{L} = \sum_{f=1}^{N_f} \bar{q}_f \left(i\gamma^\mu D_\mu - m_f \right) q_f - \frac{1}{4} Tr\, F_{\mu\nu} F^{\mu\nu}. \tag{2.17}$$

Here m_f is the mass of a quark flavor q_f and N_f denotes the number of quark flavors. The Lagrangian is invariant under the symmetry transformations of the color gauge group$SU(3)_c$. Additionally, the Lagrangian exhibits a global chiral symmetry in the massless limit of quarks. We consider only u and d quarks, the two typically light quark flavors. Further, we make a split of the quark fields in terms of their left and right-handed components

$$q_{L,R} = \frac{1}{2}(1 \pm \gamma_5)\, q. \tag{2.18}$$

Using the above and ignoring the kinetic energy term of the gauge field which is not relevant to our discussion, we write the Lagrangian as

$$\mathcal{L} = \sum_{q=u,d} \bar{q}_L \, (\, i\gamma^\mu \, D_\mu \,) q_L + \bar{q}_R \, (\, i\gamma^\mu \, D_\mu \,) q_R + m \, (\bar{q}_L q_R \, + \, \bar{q}_R q_L). \tag{2.19}$$

Here, for simplicity of calculation, we have taken the same mass m for both quarks. It is immediately apparent from the above equation that the two components of the quark field mix only through the mass term and in the massless limit the components completely decouple. This makes the Lagrangian invariant under $SU(2)_L \times SU(2)_R$ global symmetry transformations. Should the ground state (full quantum vacuum) respect the same symmetry one would expect degenerate multiplets of particles corresponding to the irreducible representations of the group $SU(2)_L \times SU(2)_R$. For instance, triplet pseudo-scalar mesons (pions) should be accompanied by their parity partners. But pions do not have such parity partners in nature. But we do see the multiplet structure of $SU(2)$ isospin in nature. Thus the vacuum of QCD must be invariant under $SU(2)$ isospin global symmetry. Therefore in QCD the $SU(2)_L \times SU(2)_R$ chiral symmetry is spontaneously broken to the $SU(2)$ isospin subgroup with the generation of Goldstone bosons as pions. However, pions are not massless; they have nonzero masses arising from nonzero masses of quarks. Thus chiral symmetry is also explicitly broken.

A simple phenomenological model which implements the idea of chiral symmetry breaking is the linear sigma model [10] originally constructed to study chiral symmetry in pion-nucleon system. The model, simple as it is, nevertheless embodies many crucial features of low-energy QCD. Here the Lagrangian is constructed out of the iso-triplet of pion $\pi = (\pi_1, \pi_2, \pi_3)$ fields and an iso-scalar σ field. The Lagrangian in terms of these fields, in the chiral limit with zero quark masses, is [11]

$$\mathcal{L} = \frac{1}{2} \left[(\partial_\mu \sigma)^2 + (\partial_\mu \pi)^2 \right] - V(\sigma, \pi), \tag{2.20}$$

with the potential $V(\sigma, \pi)$ describing the self-interaction of the scalars and is given by

$$V(\sigma, \pi) = \frac{\mu^2}{2} (\sigma^2 + \pi^2)^2 + \frac{\lambda}{24} (\sigma^2 + \pi^2)^4. \tag{2.21}$$

When the mass term μ^2 is negative the minima of the potential is given by

$$\sigma^2 + \pi^2 = -\frac{6\mu^2}{\lambda}. \tag{2.22}$$

This set of minima define the vacuum manifold $\mathcal{M}$ which is a 3-sphere S^3 in the four dimensional field space. Each point on the 3-sphere is invariant under $O(3)$, which is locally isomorphic to $SU(2)$ rotations. Thus (2.20) describes a theory in which symmetry is spontaneously broken from $O(4)$ to $O(3)$. Now, to determine the particle spectrum of the theory one has to choose a vacuum state and rewrite the fields in terms of fluctuations around it. Let our convenient choice of ground state be

$$< \sigma >= v = -\frac{6\mu^2}{\lambda}, \quad \pi = 0. \tag{2.23}$$

Expanding the sigma field around the minimum as $\sigma = v+\zeta$, the Lagrangian becomes

$$\mathcal{L} = \frac{1}{2}\left[(\partial_\mu\sigma)^2 + (\partial_\mu\pi)^2\right] + \mu^2\zeta^2 - \frac{\lambda v}{6}\zeta(\zeta^2+\pi^2) - \frac{\lambda}{24}(\zeta^2+\pi^2)^2. \tag{2.24}$$

It is now patently clear from the Lagrangian that spontaneous symmetry breaking leads to the appearance of three massless (the number of broken generators being three) pions and the radial excitation corresponding to the sigma field is massive.

To sum up, chiral symmetry is a symmetry of QCD only in the limit of zero quark masses. Current quark masses, however, are not zero. But, compared to hadronic scales, the two lightest quarks have negligible masses so that chiral symmetry may well be regarded as an approximate symmetry of QCD. Since chiral symmetry is only approximate, the pions get a finite but small mass, compared to other hadrons, in the broken phase.

2.3 Disoriented Chiral Condensate

Formation of disoriented chiral condensates (DCC) in laboratory experiments was intensively investigated some time ago. DCC refers to the formation of a chiral condensate in an extended domain, such that the direction of the condensate is misaligned from the true vacuum direction. It is expected that as the chiral field relaxes to the true vacuum in such a domain, it will lead to coherent emission of pions. A motivation for the formation of such domains came from Centauro events in cosmic ray collisions [12]. It was suggested in ref. [13] that the anomalous fluctuations in neutral to charged pion ratio observed in the Centauro (and anti-Centauro) events in cosmic ray collisions, could be due to the formation of a large region of DCC. This was termed as the *Baked Alaska* model in ref. [13]. The formation of DCC was extensively investigated in high multiplicity hadronic collisions as well as in heavy-ion collisions [13–16].

A natural framework for the discussion of the formation of DCC is the linear sigma model as this provides a simple way to model chiral symmetry restoration at high temperatures. The formation of DCC naturally happens as the temperature drops down through the critical temperature, and the chiral field picks up random directions in the vacuum manifold in different regions in the physical space. We work within the framework of linear sigma model with the Lagrangian density given by (here we will use notations as in ref. [17, 18]),

$$L = \frac{1}{2}\partial_\mu\mathbf{\Phi}\partial^\mu\mathbf{\Phi} - V(\mathbf{\Phi}, T), \tag{2.25}$$

where the finite temperature effective potential $V(\Phi, T)$ at one loop order is given by [17],

$$V = \frac{m_\sigma^2}{4}\left(\frac{T^2}{T_c^2} - 1\right)|\mathbf{\Phi}|^2 + \lambda|\mathbf{\Phi}|^4 - H\sigma. \tag{2.26}$$

Here the chiral field $\mathbf{\Phi}$ is an $O(4)$ vector with components $\mathbf{\Phi} = (\vec{\pi}, \sigma)$, and T is the temperature. We have included an explicit symmetry breaking term with coefficient H which leads to non-zero mass for pions. The values of the different parameters are taken as $m_\sigma = 600$ MeV, $\lambda \simeq 4.5$, $H = (120 \text{ MeV})^3$ and $T_c \simeq 200$ MeV, (see, ref. [18]).

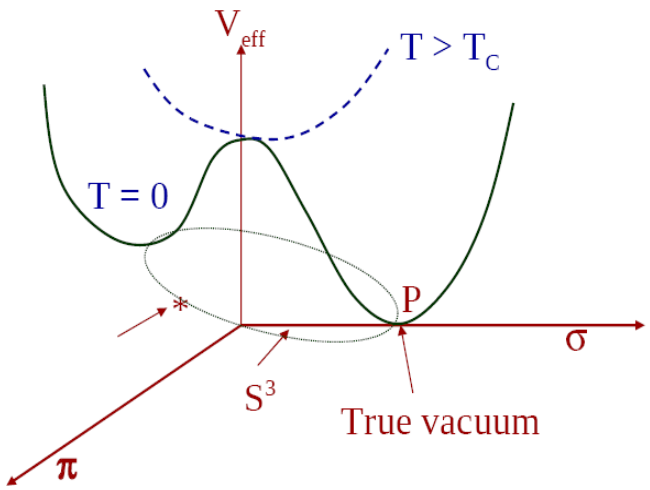

Figure 2.1: Effective potential for the chiral field $\mathbf{\Phi}$. P denotes the true vacuum on the (approximately degenerate) vacuum manifold while $*$ marks the value of the chiral field inside a DCC domain which is *disoriented* from the true vacuum direction.

In the chiral limit, spontaneous breaking of chiral symmetry (for $T < T_c$) implies that the vacuum corresponds to some specific point on the vacuum manifold S^3, with all points on S^3 being equally likely. This is not the situation in the presence of explicit symmetry breaking, as there is a unique vacuum state as shown in Fig.2.1. However, one may expect that this *preference* for the true vacuum may be insignificant during very early stages in a rapidly cooled system, due to small pion mass. Thus, as the temperature drops below T_c, one expects that the chiral field will assume some arbitrarily chosen value in the (approximately degenerate) vacuum manifold within a correlation size domain. If this value differs from the true vacuum direction (as marked by $*$ in Fig.2.1) then this domain will correspond to a DCC which will subsequently decay by emission of coherent pions as the chiral field rolls down to the true vacuum. This essentially summarizes the conventional picture of the formation of a DCC domain.

2.4 Phase Transitions

The phenomenon of phase transition is quite commonplace in everyday life, the

most familiar examples being melting of ice, boiling of water, etc. And, to cite a few examples from the laboratory, one can mention the transition from para to feromagnetic state below the Curie temperature, λ- transition of liquid He^4 from normal to superfluid phase, and transition from isotropic to nematic phase below the critical temperature in liquid crystal.

The phase of a system in equilibrium is characterized by the intrinsic parameters of the system such as temperature, volume, chemical potential etc. A diagram drawn using appropriately chosen parameters of a system give us what is known as a phase diagram. As long as a system is in a given phase in equilibrium, these parameters are analytic over the relevant part of the phase diagram. Non-analyticity of one or more of these parameters over a particular region indicates the presence of a phase boundary separating two different phases. A system always tries to minimize its free energy and this sometimes drives a system to pass over to a new phase across the phase boundary, leading to phase transition.

Often phase transitions are accompanied by a change in the symmetry properties of the system. The best example of this is theories with spontaneous symmetry breaking. In such theories the lowest energy state or ground state does not share the original symmetry of the free energy and becomes degenerate after the phase transition. While the system enjoyed a unique ground state in the symmetric phase, it now has to choose spontaneously from among the many degenerate ground states available to it and once a choice is made the system no more remains invariant to the symmetry transformations pertaining to its original unique ground state. The symmetry of the system is therefore said to be broken spontaneously during the symmetry breaking transition. Such 'ordering' phenomenon (or, spontaneous symmetry breaking) occurs in a large class of systems. The symmetric phase of a system is the disordered phase and the symmetry breaking transition makes it more ordered. But it needs to be emphasized that 'ordering' is not a necessary requirement for all transitions. For example, liquid-vapor transition does not involve any symmetry breaking or ordering since both phases are isotropic.

A useful thermodynamic variable to characterize different phases is the order parameter (OP) which is typically zero in the disordered phase enjoying higher symmetry and is nonzero in the ordered phase having lower symmetry. The values of the order parameter field which minimize the free energy in a particular phase constitute the order parameter space. In the context of quantum field theories (e.g. in the Standard model) the OP field is the Higgs field and the OP space is the vacuum manifold.

The nature of the variation of OP as a function of an appropriate controlling parameter like temperature defines the order of the phase transition. The transition is first order if the OP changes discontinuously with the control parameter; otherwise it is second order. A first order transition occurs by nucleation of bubbles. Local fluctuations of the OP field drive certain regions of one phase to the other phase because

of lower free energy of the latter. These are the bubbles which expand or collapse depending on their size and they expand if the size happens to be bigger than a critical size which can be calculated for a given system. Subcritical bubbles simply collapse. The bubbles expand, meet, and coalesce until the entire old phase gets converted to the new phase. Such moving interfaces of bubble walls lead to interesting physical effects; for example, Witten has shown that in the quark-hadron transition in the early universe, moving bubble walls can lead to concentration of baryon number and can lead to formation of quark nuggets. A classic example of first order transition is the liquid-vapour transition where density serves as order parameter. An example of second order transition is para to feromagnetic transition where magnetization (M) is the order parameter. In contrast to the above examples, there exists no fundamental order parameter for a transition like confinement-deconfinement transition in QCD, though the Polyakov loop, which captures the basic physics of the transition, can be a good order parameter.

2.5 Relativistic Heavy Ion Collisions

The aim of the relativistic heavy ion collision experiments is to create and study the properties of the QGP phase. In these experiments heavy nuclei like gold or lead are accelerated to ultra relativistic energies and are then collided. The centre of mass energies are of the order of a few hundred GeVs (or, as in LHC, in the order of TeV) per nucleon. At such high energies the quarks and gluons inside the nucleons of the colliding nuclei are essentially free due to asymptotic freedom and so they pass through each other, as if transparent. The coupling is, however, not exactly zero, and this leads to secondary particle production. The quark-gluon system in the central region of the two receding nuclei has a large energy density. These partons interact among themselves, redistribute their energy, and soon enough the system of partons reaches local thermal equilibrium. The subsequent evolution of the QGP state is described well by hydrodynamics. As the system expands it cools and when the temperature falls below the quark-hadron transition temperature, it hadronizes. Once the confinement phase transition is completed, the system consists entirely of hadrons. The hadron gas expands and while it does so rescattering among hadrons takes place, thus constantly changing the chemical composition of the system. When these inelastic scatterings become ineffective, the system undergoes chemical freeze-out. Finally comes a stage when the hadron gas gets diluted to the extent that the mean free path becomes larger than the system size thereby bringing a stop to all rescattering processes. This is the final freeze out stage; once this stage is reached the momentum distribution also does not change and the hadrons free-stream to reach the detectors. Experimentalists detect these final stage hadrons among a host of other particles such as direct photons, leptons etc.

Given the fact that what is finally observed is the hadron spectrum, the main challenge confronting experimentalists is to look for definite signatures of QGP formation in the collision process. There are a number of indicators of QGP formation; here we briefly discuss some of the important ones. One of the signals of QGP formation is the abnormal suppression of J/ψ, a $c\bar{c}$ bound state. The lifetime of the state exceeds that of the QGP; so it outlives the QGP to decay into dilepton pairs which leave the plasma without scattering and are detected in experiments. Since $c\bar{c}$ interacts with other nucleons present inside the nucleus a normal suppression is expected anyway. This expected suppression is studied in proton proton collisions and extrapolated to nucleus-nucleus collisions. However in a QGP background the force holding a $c\bar{c}$ pair is weakened because of Debye screening of color charges present in the plasma which causes $c\bar{c}$ bound states to melt away leading to suppression of J/ψ production. Similar suppression is expected of other heavy flavor quarkonium states, e.g. $b\bar{b}$ states, as well as excited states of the quarkonia.

Another signature of QGP formation is the production of dileptons and photons through the Drell-Yan process and their subsequent detection. The lepton interaction cross-section in QGP is electromagnetic and is much smaller than the strong cross-section. So the leptons produced do not further interact with the QGP and reach the detectors. Now, the rate of production and the momentum distribution of the produced l^+l^- depend on the momentum distribution of quarks and antiquarks present in the plasma which again depends on the thermodynamic condition of the plasma. Therefore, these pairs carry information about the thermodynamic condition prevailing at the time of their birth and can help us infer whether the QGP state was achieved. Likewise, photons are also produced via

$$q + \bar{q} \rightarrow \gamma + g. \tag{2.27}$$

$q\bar{q} \rightarrow \gamma\gamma$ has a smaller cross section compared to $q\bar{q} \rightarrow \gamma g$ by a factor $(\frac{\alpha_e}{\alpha_s})$. The photons, like the dileptons, do not further interact with the QGP and are therefore detected yielding more information about their birthplace.

The detection of elliptic flow, assessed by comparing the azimuthal distribution of the P_T spectra of particles with different masses, is another very useful signal which has yielded a wealth of information about the state of matter achieved at RHIC [19]. For non-central collisions the QGP formed has an initial spatial anisotropy; as a result an anisotropic pressure gradient develops which results in an anisotropic expansion of the plasma through hydrodynamic flow, which depends crucially on the equation of state relating pressure to energy density. The spatial anisotropy thus gets translated into momentum anisotropy; detection and analysis of this momentum anisotropy affords us a peek into the equation of state of the plasma. If thermalization is delayed, there would be a reduced spatial deformation and the elliptic flow would come out smaller. Recent flow results from RHIC experiment at BNL indicate the formation of a strongly coupled QGP (sQGP), with a strong non-perturbative interaction, negating

earlier expectation of formation of a weakly interacting quark-gluon gas.

There are other important probes for the detection of QGP in heavy-ion collisions, e.g. strangeness enhancement, jet quenching etc. None of the signals has provided a clear, conclusive evidence for the formation of QGP in these experiments. However, all these diverse measurements taken together lend firm support to our belief that indeed QGP is formed in relativistic heavy-ion collisions, thereby providing access to the yet uncharted domain of a new state of matter, and providing glimpses into the very high density/temperature matter which is believed to have existed in the universe during the first few microseconds of its birth.

Bibliography

[1] L. D. McLerran and B. Svetitsky, Phys. Rev. D 24, 450 (1981); L. D. McLerran, Rev. Mod. Phys. 58, 1021 (1986).

[2] R. D. Pisarski, Phys. Rev. D **62**, 111501 (2000) [hep-ph/0006205].

[3] R. D. Pisarski, hep-ph/0203271.

[4] A. Dumitru and R. D. Pisarski, Phys. Lett. B **504**, 282 (2001) [hep-ph/0010083].

[5] A. Dumitru and R. D. Pisarski, Nucl. Phys. A **698**, 444 (2002) [hep-ph/0102020].

[6] A. Dumitru and R. D. Pisarski, Phys. Rev. D **66**, 096003 (2002) [hep-ph/0204223].

[7] G. Boyd, J. Engels, F. Karsch, E. Laermann, C. Legeland, M. Lutgemeier and B. Petersson, Nucl. Phys. B **469**, 419 (1996) [hep-lat/9602007].

[8] M. Okamoto *et al.* [CP-PACS Collaboration], Phys. Rev. D **60**, 094510 (1999) [hep-lat/9905005].

[9] T. Hatsuda and T. Kunihiro, Phys. Rept. 247, 221 (1994); R.Rapp and J. Wambach, Adv. Nucl. Phys. **25**, 1 (2000).

[10] M. Gell-Mann and M. Levy, Nuovo Cimento, 16, 705 (1960).

[11] T. Cheng and L. Li, *Gauge Theory Of Elementary Particles*, (Oxford University Press), 2005.

[12] C. M. G. Lattes, Y. Fujimoto and S. Hasegawa, Phys. Rep. **65**, 151 (1980); L. T. Baradzei et al., Nucl. Phys. **B370**, 365 (1992), and references therein.

[13] J.D. Bjorken, K.L. Kowalski and C.C. Taylor, in *Results and Perspectives in Particle Physics 1993*; Proceedings of the 7th Rencontres de Physique de la Vallee d'Aoste, La Thuile, Italy, 1993, edited by M. Greco (Editions Frontieres, Gif-sur-Yvette, France, 1993).

[14] A. A. Anselm, Phys. Lett. **B217** (1989) 169; J.-P. Blaizot and A. Krzywicki, Phys. Rev. **D46** (1992) 246.

[15] J. P. Blaizot and D. Diakonov, Phys. Lett. **B315** (1993) 226.

[16] K. Rajagopal and F. Wilczek, Nucl. Phys. **B399** (1993) 395; *ibid* **B404** (1993) 577.

[17] D. Boyanovsky, H. J. de Vega, R. Holman, and S. Prem Kumar, Phys. Rev. **D 56**, 3929 (1997).

[18] A.M. Srivastava, Pramana 55, 53 (2000).

[19] Roy A. Lacey, Nucl. Phys. A774, 199 (2006).

Chapter 3

Reaction-Diffusion Equations

Our discussion so far has been on QCD in general, with emphasis on concepts such as the running coupling constant, color confinement, asymptotic freedom, prediction of QGP phase of QCD (Chapter 1), and QCD phase transitions (Chapter 2). In this chapter we take a break from QCD physics to talk about a particular class of equations of robust scope, known as the reaction-diffusion equations. This, as we shall see in the following two chapters, has a direct bearing on our work and will help put it in some perspective. We begin in section 3.1 by introducing the diffusion equation following two approaches which give complimentary insights into the nature of the equation. We follow it in the next section (3.2) with a discussion on the central theme of the chapter- the reaction-diffusion (RD) equations. Finally, we give, by way of an example and prototype, the asymptotic solution of one of the simplest types of RD equations.

3.1 The Diffusion Equation : A Mass Balance Approach

We consider for simplicity only a one-component system although the extension to multicomponent systems is straightforward. The treatment that follows can be found in any standard text on statistical mechanics, for example [1], to name just one. Let $\rho_m(\vec{r}, t)$ be the local mass density of the system at position $\vec{r}$ at time t and let $\vec{u}(\vec{r}, t)$ be the velocity of the mass. The total mass in an arbitrary fixed volume V with surface S within our fluid is

$$M = \int_V \rho_m(\vec{r}, t)\, dV. \tag{3.1}$$

The rate of change of mass in V is

$$\frac{dM}{dt} = \int_V \frac{\partial \rho_m}{\partial t}\, dV. \tag{3.2}$$

where V is fixed in space. Now, it follows from the conservation of mass that the rate of change of mass in V must be the same as the rate at which mass flows through the surface S. Since the local flow rate of mass is $\rho_m \, \vec{u}$, therefore

$$\frac{dM}{dt} = - \int_S \rho_m \, \vec{u} \cdot \vec{n} \, dS, \tag{3.3}$$

where $\vec{n}$ is a unit outward normal (local) to S. Using Gauss's divergence theorem to transform the above surface integral into a volume integral, we have

$$\frac{dM}{dt} = - \int_V \nabla \cdot (\rho_m \, \vec{u}) \, dV. \tag{3.4}$$

From equations (2) and (4) we have

$$\int_V \left[\frac{\partial \rho_m}{\partial t} \, + \, \nabla \cdot (\rho_m \, \vec{u}) \right] \, dV = 0. \tag{3.5}$$

Since V is arbitrary, we must have

$$\frac{\partial \rho_m}{\partial t} \, + \, \nabla \cdot (\rho_m \, \vec{u}) = 0. \tag{3.6}$$

This is the well known equation of continuity for mass. By using the vector identity

$$\nabla \cdot (a \, \vec{u}) = a \, \nabla \cdot \vec{u} + \vec{u} \cdot \nabla a \, , \tag{3.7}$$

we can rewrite the above in the form

$$\frac{D \rho_m}{Dt} + \rho_m \, \nabla \, \cdot \vec{u} = 0, \tag{3.8}$$

where the derivative

$$\frac{D}{Dt} = \frac{\partial}{\partial t} \, + \, \vec{u} \, \cdot \nabla, \tag{3.9}$$

occurs frequently in continuum mechanics and is known as the hydrodynamic derivative, or the substantial derivative, or the Stokes' operator.

We now apply equation (3.6) to a special case where we assume that the rate of flow of mass is proportional to the gradient of the density. This is known as Fick's law of diffusion, an empirical law valid when the gradient of the density is small. Put mathematically, the law simply states

$$\rho_m \, \vec{u} = - \, D \, \mathrm{grad} \, \rho_\mathrm{m}, \tag{3.10}$$

Where D is known as the diffusion constant, not to be confused with the operator D introduced above. Substituting this into the equation of continuity we arrive at the diffusion equation

$$\frac{\partial \rho_m}{\partial t} = D \, \nabla \cdot (\nabla \, \rho_m) = D \, \nabla^2 \, \rho_m. \tag{3.11}$$

True to its name, the diffusion equation is generally applied to the diffusion of one species through some medium and with this very specific use in mind it is usually cast in the form

$$\frac{\partial c}{\partial t} = D\,\nabla^2\,c, \tag{3.12}$$

where c is the concentration of the diffusing species. The solution to this equation depends upon the initial distribution of concentration and the geometry of the boundary confining the system. The solution is, therefore, case-specific. However, it turns out that solution for any geometry and initial conditions can be built up out of a fundamental solution that applies to diffusion in an infinite medium (i.e. no boundaries) with the diffusing substance initially concentrated at the origin. This solution is thus the Green's function of the diffusion equation.

To develop a feel for such solutions we consider the simple situation of isotropic diffusion in three dimensions in spherical polar coordinates. The diffusion equation, to repeat, is

$$\frac{\partial c}{\partial t} = D\,\nabla^2\,c, \tag{3.13}$$

and the initial condition is

$$c(\,\vec{r},\,0) = c_0\,\delta(\vec{r}), \tag{3.14}$$

where $\delta(\vec{r})$ is the 3-d Delta function centred at the origin.

We define a three-dimensional Fourier transform of $c(\vec{r},\,t)$ in the following way

$$\hat{C}(\,\vec{k},\,t) = (2\,\pi)^{-\,3/2}\int_{-\infty}^{\infty}\int_{-\infty}^{\infty}\int_{-\infty}^{\infty} e^{i\,\vec{k}\cdot\vec{r}}\,c(\,\vec{r},\,t)\,d^3\vec{r}, \tag{3.15}$$

the inverse of which is

$$c(\,\vec{r},\,t) = (2\,\pi)^{-\,3/2}\int_{-\infty}^{\infty}\int_{-\infty}^{\infty}\int_{-\infty}^{\infty} e^{-i\,\vec{k}\cdot\vec{r}}\,\hat{C}(\,\vec{k},\,t)\,d^3\vec{k}. \tag{3.16}$$

Hence

$$\mathrm{grad}\,c(\,\vec{r},\,t) = -\frac{i}{(2\,\pi)^{\,3/2}}\int_{-\infty}^{\infty}\int_{-\infty}^{\infty}\int_{-\infty}^{\infty}\vec{k}\,e^{-i\,\vec{k}\cdot\vec{r}}\,\hat{C}(\,\vec{k},\,t)\,d^3\vec{k}, \tag{3.17}$$

and

$$\begin{aligned}\mathrm{div}\,\mathrm{grad}\,c(\,\vec{r},\,t) &= \nabla^2 c(\,\vec{r},\,t)\\ &= -\frac{1}{(2\,\pi)^{\,3/2}}\int_{-\infty}^{\infty}\int_{-\infty}^{\infty}\int_{-\infty}^{\infty}k^2\,e^{-i\,\vec{k}\cdot\vec{r}}\,\hat{C}(\,\vec{k},\,t)\,d^3\vec{k}\\ &.\end{aligned} \tag{3.18}$$

Thus if we take the Fourier transform of (3.13), we get

$$\frac{\partial\hat{C}(\vec{k},t)}{\partial t} = -D\,k^2\,\hat{C}(\vec{k},t)\,, \tag{3.19}$$

with the initial condition

$$\hat{C}(\,\vec{k},\,0) = (2\,\pi)^{-\,3/2}\,c_0 = \hat{C}_0. \tag{3.20}$$

The solution to (3.19) is

$$\hat{C}(\,\vec{k},\,t) = \hat{C}_0\, e^{-D\,k^2\,t}. \tag{3.21}$$

Taking inverse of (3.21) we get

$$\begin{aligned} c(\,\vec{r},\,t) &= (2\,\pi)^{-\,3/2} \int_{-\infty}^{\infty}\int_{-\infty}^{\infty}\int_{-\infty}^{\infty} e^{-i\,\vec{k}\cdot\vec{r}}\,\hat{C}(\,\vec{k},\,t)\,d^3\vec{k}, \\ &= c_0\,(2\,\pi)^{-3} \int_{-\infty}^{\infty}\int_{-\infty}^{\infty}\int_{-\infty}^{\infty} e^{-i\,\vec{k}\cdot\vec{r}}\,e^{-D\,k^2\,t}\,d^3\vec{k}, \\ &= \frac{c_0}{8\,(\pi\,D\,t)^{3/2}}\,e^{-\,r^2\,/4\,D\,t}. \end{aligned} \tag{3.22}$$

This is the well-known solution to the diffusion equation and shows that the diffusing material, initially concentrated at the origin, spreads out in time such that the Gaussian profile of concentration, initially sharply peaked at the origin, flattens with time. As a check one can verify that

$$\int_0^{\infty} c(r,t)\,4\,\pi\,r^2\,dr = c_0. \tag{3.23}$$

Finally, the solution to the one-dimensional diffusion equation can be shown to be

$$c\,(\,x,\,t) = \frac{c_0}{2\,(\pi\,D\,t)^{1/2}}\,e^{-\,x^2\,/4\,D\,t}. \tag{3.24}$$

We shall refer to this in the next section.

3.2 The Diffusion Equation : A statistical Approach

In our derivation of the diffusion equation we adopted a macroscopic approach in that we did not concern ourselves with the dynamics of the diffusion process ; the individual behaviour of the diffusing particles was completely ignored. In the present section we continue to maintain our indifference to the individual and focus instead on their collective behaviour from a probabilistic point of view. We show that such an approach [2], though different in spirit from the previous one, nevertheless lands us, quite remarkably, with the same equation .

In an assemblage of particles such as a concentration of cells, chemicals, elementary particles,...etc, each particle moves about randomly and spread out as a result of such individual motion. However, if such random, uncorrelated movement, results in some gross regular motion of the group we can think of it as a *diffusion* process. Of course there can be interaction among the particles and the environment can bias the mass movement but for the time being we neglect such effects.

To start with we consider a simple one-dimensional random walk process. Consider a particle moving randomly backward and forward along the x axis in steps of $\triangle x$, each taken in a fixed time $\triangle t$. We want the probability $p(m,\, n)$ that a particle reaches a point m space steps to the right (that is, to $x = m \triangle x$) after n time-steps (that is, after a time $n \triangle t$). Suppose that this is achieved by taking a steps to the right and b steps to the left. Then

$$m = a - b, \qquad a + b = n \qquad \Rightarrow \quad a = \frac{n+m}{2}, \quad b = n - a. \tag{3.25}$$

The number of possible paths is

$$C_a^n = \frac{n!}{a!\,(n-a)\,!} = \frac{n!}{a!\,b!}. \tag{3.26}$$

The total number of possible n-steps being 2^n, the probability $p(m,\, n)$ is

$$p(m,\, n) = \frac{1}{2^n}\,\frac{n!}{a!\,(n-a)\,!}\,, \tag{3.27}$$

with $n + m$ even. We notice that

$$\sum_{m=-\,n}^{n} p(m,\, n) = 1\,, \tag{3.28}$$

being the sum of all probabilities, and $p(m,\, n)$ is the *binomial distribution*. If we now allow both m and n to be large and use Stirling's formula

$$n! \sim (\,2\,\pi\,n\,)^{1/2}\,n^n\,e^{-n}, \quad n \gg 1 \tag{3.29}$$

in (3.27), we get the *normal* or *Gaussian probability distribution*. Now set

$$m \triangle x = x, \qquad n \triangle t = t, \tag{3.30}$$

where x and t are continuous space and time variables. Further, let $m \to \infty$, $n \to \infty$, $\triangle x \to 0$, $\triangle t \to 0$, keeping x and t finite. Then the appropriate dependent variable is ; $u = p\,/\,(2 \triangle x)$; $2\,u \triangle x$ is the probability that the particle is in the interval $(\,x, x + \triangle x)$ at time t. So (3.27) becomes

$$\frac{p\,(\,\frac{x}{\triangle x}, \frac{t}{\triangle t}\,)}{(2 \triangle x)} \;\sim\; \left\{\frac{\triangle t}{2\,\pi\,t\,(\triangle x\,)^2}\right\}^{1/2} \exp\left\{-\frac{x^2}{2\,t}\,\frac{\triangle t}{(\triangle x\,)^2}\right\}. \tag{3.31}$$

Also, assume

$$\lim_{\triangle x \to 0,\, \triangle t \to 0} \frac{(\triangle x)^2}{2 \triangle t} = D \neq 0. \tag{3.32}$$

Hence

$$u\,(\,x,\,t\,) = \lim_{\triangle x \to 0,\, \triangle t \to 0} \frac{p\,(\,\frac{x}{\triangle x}, \frac{t}{\triangle t}\,)}{(2 \triangle x)} = \left(\frac{1}{4\,\pi\,D\,t}\right)^{1/2} e^{-\,x^2\,/(4\,D\,t)}, \tag{3.33}$$

where D is the *diffusion coefficient* or *diffusivity* of the particles. The above expression gives us the probability that a particle released at $x = 0$ at $t = 0$ reaches x in time t. At time $(t - \triangle t)$ the particle was at $(x - \triangle x)$ or $(x + \triangle x)$. With α and β as the probabilities for the particle to move to the right or left respectively, we have

$$p(\,x, t\,) = \alpha\, p\,(x - \triangle x, t - \triangle t\,) + \beta\, p\,(x + \triangle x, t - \triangle t\,), \quad \alpha + \beta = 1. \tag{3.34}$$

For an unbiased random walk $\alpha = \beta = 1/2$. A Taylor series expansion of the right hand side of the above expression gives us

$$\frac{\partial\, p}{\partial\, t} = \left[\frac{(\triangle x)^2}{2\triangle t}\right] \frac{\partial^2 p}{\partial\, x^2} + \left(\frac{\triangle t}{2}\right) \frac{\partial^2 p}{\partial\, t^2} + \ldots\ldots \tag{3.35}$$

If again we let $\triangle x \to 0$, $\triangle t \to 0$ and define D as before we get

$$\frac{\partial p}{\partial t} = D\, \frac{\partial^2 p}{\partial\, x^2}. \tag{3.36}$$

If the total number of particles released be Q, then the particle concentration $c(\,x, t\,) = Q\, p(\,x, t\,)$ and we recover from the last equation the one-dimensional diffusion equation.

3.3 Reaction-Diffusion Equations

Having obtained some insight into how the diffusion equation can arise in realistic situations, we are now in a position to comment on some limitations of the equation, while, of course, not denying the equation of its obvious usefulness. An order of magnitude estimate of the typical time to convey information in the form of a changed concentration over a distance L is $O\,(L^2/D\,)$. Such an estimate can be made from the solution itself (3.24), dimensional arguments, or similarity solutions. It is oftentimes found that the order of time so obtained is excessively long, contrary to reality, for many processes in real-life situations. The inescapable conclusion is diffusion is unlikely to be the only vehicle for disseminating information over significant distances. In contrast we shall show presently that if reaction kinetics and diffusion are coupled, travelling waves of concentration can exist and and can affect concentration in a way much faster than diffusion-driven processes governed by the diffusion equation alone. Now, the diffusion equation is one of a class of equations known as linear parabolic equations the theory of which show that there are no physically realistic travelling wave solutions. To appreciate this point, assume, for instance, a travelling wave solution of the form

$$u(\,x, t\,) = u(\,x - ct\,) = u(\,z\,), \quad z = x - c\,t. \tag{3.37}$$

Note that we are denoting concentration by u, rather than c, to reserve c to denote wave speed. The diffusion equation becomes

$$D\, \frac{d^2 u}{dz^2} + c\, \frac{du}{dz} = 0 \quad \Rightarrow \quad u(z) = A + B\, e^{-c\, z/D}, \tag{3.38}$$

where A, B are integration constants. Now, since u has to be bounded for all z, B must be zero, otherwise the exponential part of the solution blows up as $z \to -\infty$. Therefore, $u(z) = A$, a constant, is not a wave solution. In sharp contrast we shall see that reaction-diffusion equations can accommodate travelling wave solutions, depending on the nature of interaction / reaction.

We now give a formal derivation of reaction-diffusion equations [2]. To that end, we consider diffusion in three dimensions. Consider an arbitrary volume V in a medium bounded by the surface S. Conservation principles require that the rate of change of matter content in V is equal to the rate at which matter flows out of or into V through S plus the rate of creation/destruction of matter in V. Thus

$$\frac{\partial}{\partial t} \int_V c(\vec{x}, t)\, dv = -\int_S \vec{J} \cdot d\vec{s} + \int_V f\, dv, \tag{3.39}$$

where $\vec{J}$ is the flux of material and f, which in the most general situation can be a function of c, $\vec{x}$, and t, represents the source / sink of material. Applying the divergence theorem to the surface integral and assuming $c(\vec{x}, t)$ to be continuous, the above equation becomes

$$\int_V \left[\frac{\partial c}{\partial t} + \nabla \cdot \vec{J} - f(c, \vec{x}, t) \right] dv = 0. \tag{3.40}$$

Since the above relation is true for any volume V the integrand must be zero and so we get the conservation equation for c as

$$\frac{\partial c}{\partial t} + \nabla \cdot \vec{J} = f(c, \vec{x}, t). \tag{3.41}$$

This equation is universal in that it holds for a general flux transport $\vec{J}$, whatever be the process.

If the process under study is diffusion then we have the following three dimensional generalization of Fick's law

$$\vec{J} = -D \nabla c, \tag{3.42}$$

and (3.41) becomes

$$\frac{\partial c}{\partial t} = f + \nabla \cdot (D \nabla c), \tag{3.43}$$

where D may be a function of $\vec{x}$ and c and f a function of c, $\vec{x}$, and t. This, then, is the reaction-diffusion equation we set out to derive.

The above equation may be further generalized to systems consisting of several interacting species or chemicals or particles. To handle such multi-component systems we introduce a vector $u_i(\vec{x}, t), \quad i = 1, \cdots, m$ of concentrations or densities, each characterized by its own diffusion coefficient D_i and interacting according to the vector source term $\vec{f}$. The reaction-diffusion equation (3.43)then generalizes to

$$\frac{\partial \vec{u}}{\partial t} = \vec{f} + \nabla \cdot (D \nabla \vec{u}) \tag{3.44}$$

where D is a matrix of diffusivities and if cross diffusivities are small then this matrix is essentially a diagonal matrix. Our purpose is in fact quite well served by equations with D diagonal and $\vec{f}$ a function only of u. We note that $\nabla\vec{u}$ is a tensor so $\nabla \cdot (D \nabla \vec{u})$ is a vector.

There exists in the literature a rich variety of reaction-diffusion equations, each with its respective area(s) of applicability. However we mention here only three of them - the first one because of its pedagogical importance, among others, and the other two because of their relevance to our work. They are [3] :

• The Fisher-Kolmogoroff equation or logistic equation

$$U_t = U_{xx} + u\,(1-u) \tag{3.45}$$

which serves as a deterministic model for the spread of an advantageous gene in a population.

• The Newell- Whitehead equation or amplitude equation

$$U_t = U_{xx} + u\,(1-u^2) \tag{3.46}$$

which arises in the study of thermal convection of a fluid heated from below.

• The Nagumo equation or bistable equation

$$U_t = U_{xx} + u\,(1-u)\,(u-a) \quad \text{with} \quad 0 < a < 1, \tag{3.47}$$

which arises as one of a set of equations modeling the transmission of electrical pulses in a nerve axon.

3.4 Fisher-Kolmogoroff Equation and Propagating Wave Solutions

The Fisher-Kolmogoroff equation

$$\frac{\partial u}{\partial t} = k\,u\,(1-u) + D\,\frac{\partial^2 u}{\partial x^2}, \tag{3.48}$$

where k and D are positive parameters is one of the simplest nonlinear reaction-diffusion equations and serves as a prototype equation admitting travelling wavefront solutions. To investigate the existence and form of travelling wave solutions, it is advantageous to rescale equation (3.48) by introducing [2]

$$t^* = k\,t, \quad x^* = x\left(\frac{k}{D}\right)^{1/2}, \tag{3.49}$$

and omitting the asterisks for simplicity, (3.48) becomes

$$\frac{\partial u}{\partial t} = u\,(1-u) + \frac{\partial^2 u}{\partial x^2}. \tag{3.50}$$

In a spatially homogeneous situation the steady state corresponds to $u = 0$ and $u = 1$ which are respectively unstable and stable. Hence we look for travelling wave solutions for which $0 \leq u \leq 1$, negative u being devoid of any physical meaning.

Any travelling wave takes the following form

$$u\,(x,t) = U(z), \quad z = x - c\,t, \tag{3.51}$$

where c is the speed of the wave. Since (3.48) is invariant under x going to $-x$, c may be positive or negative. We take $c \geq 0$. On substituting (3.51) into (3.50), $U(z)$ satisfies

$$U'' + c\,U' + U\,(1-U) = 0, \tag{3.52}$$

where prime denotes differentiation with respect to z. Our task is to find the value or values of the eigenvalue c such that a non-negative solution of (3.52) exists for which

$$\lim_{z\to\infty} U(z) = 0, \qquad \lim_{z\to-\infty} U(z) = 1. \tag{3.53}$$

Fisher found that (3.52) admits an infinite number of travelling wave solutions with wave speeds

$$c \geq c_{\min} = 2, \tag{3.54}$$

and in terms of the original variables

$$c \geq c_{\min} = 2\,(k\,D)^{1/2}. \tag{3.55}$$

3.5 Asymptotic Travelling Wave Solution to the Fisher-Kolmogoroff Equation

We have seen that there exists travelling wavefront solutions $U(z)$ for equation (3.50) which satisfy (3.52) with $U(-\infty) = 1$ and $U(\infty) = 0$, for all wavespeeds $c \geq 2$. Although no analytical solution for general c has been found, the equations do have a small parameter, namely, $\epsilon = \frac{1}{c^2} \leq 0.25$, which suggests we look for asymptotic solutions for $0 < \epsilon \ll 1$. Since the wave solutions are invariant under a shift in the origin of the coordinate system (i.e. the equation remains unchanged if $z \to z +$ constant), let us take $U = 1/2$ to be at $z = 0$. We now use a standard singular perturbation technique [2,4]. To that end, we introduce a change of variable in the vicinity of the front in a way that we can express the solution as a Taylor expansion in the small parameter ϵ. Under the transformation

$$U(z) = g(\xi), \quad \xi = \frac{z}{c} = \epsilon^{1/2}\,z, \tag{3.56}$$

equation (3.52) becomes

$$\epsilon \frac{d^2 g}{d\xi^2} + \frac{dg}{d\xi} + g\,(1-g) = 0, \tag{3.57}$$

and the boundary conditions on U become

$$g(-\infty) = 1, \quad g(\infty) = 0, \quad 0 < \epsilon \leq \frac{1}{c^2_{\min}} = 0.25, \tag{3.58}$$

with the additional requirement $g(0) = 1/2$.

We now look for solutions of (3.57) as a perturbation series in ϵ. Let

$$g\,(\xi;\epsilon) = g_0\,(\xi) + \epsilon\, g_1\,(\xi) + \cdots . \tag{3.59}$$

The boundary conditions at $\pm\infty$ and our choice that $U(0) = 1/2$, which requires that $g(0;\,\epsilon) = 1/2$ for all ϵ, gives us the following conditions

$$g_0(-\infty) = 1, \quad g_0(\infty) = 0, \quad g_0(0) = \frac{1}{2}, \tag{3.60}$$

and

$$g_i(\pm\infty) = 0, \quad g_i(\infty) = 0, \quad \text{for} \quad i = 1,\, 2,\, \cdots . \tag{3.61}$$

Substituting equation (3.59) into (3.57) and equating powers of ϵ we get

$$O(1): \quad \frac{dg_0}{d\xi} = -g_0\,(1-g_0) \quad \Rightarrow g_0(\xi) = \frac{1}{1+\epsilon^{\xi}}, \tag{3.62}$$

and

$$O(\epsilon): \quad \frac{dg_1}{d\xi} + g_1\,(1-2\,g_0) = -\frac{d^2 g_0}{d\xi^2}, \tag{3.63}$$

and likewise for higher orders in ϵ The constant of integration in the g_0-equation was so chosen that $g_0(0) = 1/2$ is satisfied. Using equation (3.62), equation (3.63) becomes

$$\frac{dg_1}{d\xi} - \left(\frac{g_0''}{g_0'}\right) g_1 = -\,g_0'', \tag{3.64}$$

which on integration and using the conditions (62) and (63) gives

$$g_1 = -g_0' \ln\left[4 \mid g_0' \mid\right] = \epsilon^{\xi}\,\frac{1}{(1+\epsilon^{\xi})^2} \ln\left[\frac{4\,\epsilon^{\xi}}{(1+\epsilon^{\xi})^2}\right]. \tag{3.65}$$

Re-introducing U and z we have

$$U(z;\,\epsilon) = (1+e^{z/c})^{-1} + \frac{1}{c^2}\,(1+e^{z/c})^{-2} \ln\left[\frac{4\,e^{z/c}}{(1+e^{z/c})^2}\right] + O\left(\frac{1}{c^4}\right), \quad c \geq c_{\min} = 2. \tag{3.66}$$

Comparison with numerical solutions reveal that the above solution is least accurate for $c = 2$.

We have so far tried to give a flavour of reaction-diffusion equations as a class of extremely robust equations with a wide applicability. Having laid the groundwork, we are now in a position to show how specific types of reaction-diffusion equations can be profitably applied to QGP scenarios. That will be the subject of our next two chapters.

Bibliography

[1] Donald A. McQuarrie, *Statistical Mechanics*, (Harper and Row), 1976.

[2] J.D.Murray, *Mathematical Biology, I : An Introduction, Third Edition*, (Springer), 2002; J.D.Murray, *Lectures on Nonlinear-Differential-Equation Models in Biology*, (Clarendon Press), 1977.

[3] B.H.Gilding and R.Kersner, *Travelling Waves in Nonlinear Diffusion Convection Reaction*, (Springer Basel AG, Switzerland), 2004.

[4] B.Bradshaw-Hajek, *Reaction-diffusion Equations for Population Genetics*, (Ph.D. thesis, School of Mathematics and Applied Statistics, University of Wollongong), 2004, (http://ro.uow.edu.au/thesis/201).

Chapter 4

Reaction-Diffusion Equation for Quark-Hadron Transition in Heavy-Ion Collisions

Our objective so far has been to present the concepts and tools we make use of in our work. That being done, we are finally in a position to present our own work. This section aims to put our work in a perspective. In sections 4.1 and 4.2 we apply a particular type of reaction-diffusion equation to chiral symmetry breaking transition and show that the transition is completed by a propagating interface. Sections 4.3 and 4.4 continue in the same spirit and present similar results obtained by applying another type of reaction diffusion equation to confinement deconfinement phase transition. In section 4.5 we discuss certain implications of our results for the chiral transition and C-D transition. The final section summarizes our results; it also talks about the implication of these results for heavy-ion collisions and the early universe.

The dynamics of the quark hadron transition is one of the most important issues in relativistic heavy-ion collisions, as well as in the universe. Earlier it used to be believed that the quark-hadron transition is first order even at low chemical potential (as in the early universe). This led to a very important proposal by Witten [1] about the possibility of the formation of quark nuggets due to the concentration of quarks by moving phase boundaries at the quark-hadron transition. The dynamics of first order transition also had important implications for heavy-ion collisions [2]. Subsequently, lattice results showed that the quark-hadron transition is not first order; rather, it is most likely a cross-over for low chemical potential. This cross-over is believed to govern the dynamics of transitions in relativistic heavy-ion collisions at high energies. (Although for lower energies, transitions may become first order when the baryonic chemical potential is sufficiently large.)

For the dynamics of the phase transition, the most important difference between

a first-order transition and a cross-over (or a continuous transition) is the presence of a phase boundary for the former case which separates the two phases. The transition for a first order case is completed by nucleation of bubbles which expand. The moving bubble walls (phase boundaries) lead to physical phenomena, such as non-trivial scattering of quarks, local heating, specific types of fluctuations, etc., which are qualitatively different from the case of a cross-over or a continuous transition.

It turns out that the presence of moving interfaces is more generic, and not necessarily restricted to the case of first order transitions. Such situations routinely arise in the study of so called *reaction-diffusion equations* [3, 4], typically studied in the context of biological systems, e.g. population genetics, and chemical systems. A typical solution of such equations, with appropriate boundary conditions, consists of a traveling front with well defined profile, quite like the profile of the interface in a first order transition case. The importance of these traveling fronts in the context of high energy physics has been recognized relatively recently in several works [5]. In the present work we demonstrate such solutions for chiral phase transition and confinement-deconfinement (C-D) transition in QCD even when the underlying transition is a cross-over or a continuous transition. The only difference between the field equations in relativistic field theory case and the reaction-diffusion case is the absence of second order time derivatives in the latter case. Thus,the correspondence between the two cases is easily established in the presence of a strong dissipation term, leading to a dominant first order time derivative term. Further, we show that the required boundary conditions for the existence of such a *traveling front* naturally arise in the context of relativistic heavy-ion collision experiments (RHICE). For the case of the universe also it may happen in special situations as we will discuss below.

We would like to clarify that the propagating front we consider here is like a phase boundary (as in a first-order transition), and has nothing to do with hydrodynamic flow. So, the front will still move, converting one phase (say, a chirally symmetric phase) to the other phase (chiral-symmetry-broken phase) even if the plasma is completely static. However, the QGP produced in RHICE undergoes hydrodynamic expansion for which one can use either Bjorken's boost-invariant scaling model for longitudinal expansion, or a three-dimensional expansion expected to be applicable at the late stages of plasma evolution. These are incorporated simply by using appropriate metrics for the field equations and they lead to a term of the form $\frac{\dot{\phi}}{\tau}$ where the time derivative is with respect to the proper time τ. It remains to be explored how this new type of phase transition dynamics can be incorporated in studies of full relativistic hydrodynamical evolution of the plasma.

We will see that the timescale for the phase conversion by the propagation of the front can easily be of order of several fm. Such a large timescale for a propagating front will be hard to accommodate even for a chiral-symmetry-breaking transition at late stages, and there is clearly no room for such timescales for the initial confinement-deconfinement transition (e.g. it would be in direct conflict with elliptic-flow data). Thus the main lesson from our results will be that at least some part of the transition dynamics is likely to be controlled by such propagating fronts, which are just like

first-order interfaces. Observational constraints then have to be used to constrain the period of such types of dynamics and then discuss how some other *faster* processes of phase conversion should take over. We will briefly discuss such *alternate* processes of phase conversion, e.g. incorporating short-wavelength fluctuations in section III.A.

There is a wide veracity of reaction-diffusion equations, see, e.g. ref. [3, 4]. We discuss specific equations which can be identified with the field equations for the chiral transition and the C-D transition in QCD in strong dissipation limit. Subsequently, we discuss different situations in the context of RHICE, with realistic dissipation, and show that propagating front solutions of these equations still persist, making the dynamics of the relevant transitions effectively like a first-order phase transition.

4.1 Reaction-Diffusion Equation for Chiral Transition

From the form of these reaction-diffusion equations it will be clear that such traveling-front solutions will exist when the underlying potential allows for a non-zero order parameter in the vacuum state, along with a local maximum of the potential [3,4]. The corresponding values of the order parameter provide the required boundary conditions for the propagating-front solution. First we consider the case of a spontaneous chiral-symmetry-breaking transition for the two-flavor case with the chiral order parameter being the O(4) field $\phi = (\sigma, \vec{\pi})$. We consider the situation in the context of RHICE, and study the transition from a chiral symmetry (approximately) restored phase to the chiral-symmetry-broken phase when the partonic system hadronizes during the evolution of a QGP. For the plasma evolution at this stage, we consider longitudinal expansion as well as spherical expansion (which may be more appropriate for late stages of hadronization). The field equations are [6]:

$$\ddot{\phi} - \bigtriangledown^2\phi + \eta\dot{\phi} = -4\lambda\phi^3 + m(T)^2\phi + H,$$
$$m(T)^2 = \frac{m_\sigma^2}{2}(1 - \frac{T^2}{T_c^2}). \tag{4.1}$$

Here, ϕ is taken along the σ direction. T is the temperature and time derivatives are with respect to the proper time τ. We have characterized the dissipation term here in terms of η, which is not a constant for an expanding plasma. For the Bjorken one-dimensional scaling case $\eta = 1/\tau$, while for the spherical expansion $\eta = 3/\tau$. We again mention that we are only using field equations in the background of an expanding plasma where expansion is incorporated by using time-dependent background metric. It will be interesting to study this phase transition dynamics in full relativistic hydrodynamical evolution of the plasma. The values of different parameters are taken [6], $\lambda = 4.5, m_\sigma = 600$ MeV, and $T_c = 200$ MeV. The coefficient of the explicit symmetry breaking term $H = (120MeV)^3$. In the chiral limit there is a second-order phase transition with the critical temperature T_c. In view of the explicit

symmetry-breaking term we take $T = 150$ MeV which allows for the presence of the central maximum in the effective potential.

To establish exact correspondence with the reaction-diffusion equation, we first neglect explicit breaking of chiral symmetry (i.e. $H = 0$ in Eq.(4.1)). Let us also consider the extreme dissipative case of large value of η which is time independent, and neglect the $\ddot{\phi}$ term. For the resulting equation, we rescale the variables as follows: $x \to m(T)x$, $\tau \to \frac{m(T)^2}{\eta}\tau$, and $\phi \to 2\frac{\sqrt{\lambda}}{m(T)}\phi$. The resulting equation is,

$$\dot{\phi} = \bigtriangledown^2\phi - \phi^3 + \phi. \tag{4.2}$$

This equation, in one dimension with $\bigtriangledown^2\phi = d^2\phi/dx^2$, is exactly the same as the reaction-diffusion equation known as the Newell-Whitehead equation [3,4]. The term $d^2\phi/dx^2$ is the diffusion term while the other term on the right hand side of Eq.(4.2) is the so called *reaction term* (representing the reaction of members of biological species for biological systems). We will briefly recall the analytical traveling front solutions for the Newell-Whitehead equation for the present case. Subsequently we will study the solutions numerically which will help us in obtaining traveling-front solutions while retaining the $\ddot{\phi}$ (and with η being time dependent as for the expanding plasma).

4.2 Propagating-Front Solutions for Chiral Transition

4.2.1 Analytical Solution

Non-trivial traveling front solutions for the Newell-Whitehead equation arise when suitable boundary conditions are imposed; namely, $\phi = 0$ and 1 at $x \to \pm\infty$. The analytical solution with these boundary conditions has the form

$$\phi(z) = [1 + exp(z/\sqrt{2})]^{-1}, \tag{4.3}$$

where $z = x - v\tau$. v is the velocity of the front [4] and has the value $v = 3/\sqrt{2}$ for this solution. The reaction-diffusion equations typically have several solutions, each with different propagation speeds [4]. For example, Eq.(4.2) also has a static solution of the form $tanh(z)$. Such a solution can have very important implications for RHICE as well as for cosmology. We will later briefly comment on it. For now we continue with the above analytical solution (Eq.(4.3)). In Fig.4.1a we show the propagation of this front. For this we have solved Eq.(4.2) by using the leapfrog algorithm of second-order accuracy. We have also added the second-order time derivative for the numerical solution of Eq.(4.2) for numerical stability and also for comparison with solutions of the full Eq.(4.1). The requirement of dissipation-dominated dynamics is fulfilled by keeping the η coefficient of $\dot{\phi}$ term large, with constant $\eta = 10$ fm^{-1}. This

introduces a simple scaling of velocity by a factor $1/\eta$. The solid curve in Fig.4.1a shows the initial profile of the analytical solution in Eq.(4.3). Plots at subsequent times show the propagation of the front. The velocity of the front is numerically obtained directly by determining the velocity of the front (specifically a particular point on the front, say $\phi = 0.5\phi_{max}$). We find $v = 0.21$ for $\eta = 10$ fm^{-1}, in complete agreement with the scaled velocity $v = \frac{1}{\eta}\frac{3}{\sqrt{2}}$.

For the case of chiral-symmetry-breaking transitions in relativistic heavy-ion collisions, the boundary conditions required for the solution of Eq.(4.2) naturally arise due to radial profile of the energy density of the plasma. The center of plasma represents the highest temperature T_{cntr} which smoothly decreases to values less than the chiral transition temperature T_c in the outer regions of the plasma. Thus, at any time when $T_{cntr} > T_c$, the chiral field will take a chirally (approximately) symmetric value (which will be zero when $H = 0$) at the center $r = 0$ and will take a symmetry-broken value at large distances. We take such an initial profile, and evolve it when T_{cntr} also reduces to a temperature T_0 below T_c. For simplicity, we assume T_0 to be uniform over the range of the profile of ϕ with ϕ in the center of the plasma having a value ϕ_0 (corresponding to the central maximum of the potential at $T = T_0$). ϕ in outer regions of the plasma will take the vacuum expectation value ξ for $T = T_0$. With such boundary conditions, the analytical solution in Eq.(4.3), written in terms of the original (unscaled) field and of the parameters of Eq.(4.1), takes the form,

$$\phi(z) = \xi[1 + exp(\frac{m(T)}{\sqrt{2}}(x - v\tau))]^{-1}, \tag{4.4}$$

where $\xi = \frac{m(T)}{2\sqrt{\lambda}}$ is the vacuum expectation value of ϕ (for $H = 0$) and the velocity becomes $v = \frac{3m(T)}{\eta\sqrt{2}}$. Interestingly, the profile of this analytical solution is similar to the Woods-Saxon form. From the energy density profile expected for colliding heavy nuclei, a Woods-Saxon-type profile for the field is rather natural.

It turns out that the form of the traveling front, and its evolution, is essentially unaffected even if we use a nonzero value of H in Eq.(4.1). Thus, we calculate the numerical profile of the front using a nonzero value of $H = (120MeV)^3$. This changes the boundary conditions for $\phi(z)$. For parameter choice in Eq.(4.1), the vacuum expectation value of ϕ is found to be $\xi = 75.18$ MeV while the central maximum of the potential is shifted to $\phi = \phi_0 =$ -25.93 MeV. The above analytical solution in Eq.(4.4), suitably modified for these changed boundary conditions, becomes,

$$\phi(z) = -\frac{(\xi - \phi_0)}{A_0}[1 + exp(\frac{m(T)(|z| - R_0)}{\sqrt{2}})]^{-1} + \xi, \tag{4.5}$$

where the normalization factor $A_0 = [1 + exp(\frac{-m(T)R_0}{\sqrt{2}}]^{-1}$. Here we use $|z|$ in order to have a symmetric front on both sides of the plasma for the present one-dimensional (1D) case. R_0 represents the width of the central part of the plasma.

We come back now to the issue of the time-scale of phase conversion as briefly discussed at the end of the introduction. The expression of the velocity of the front $v \sim \frac{m(T)}{\eta}$ for the extreme-dissipation-dominated case ($\eta \to \infty$) implies that the timescale

of phase conversion diverges in the large-volume limit, which is clearly unphysical. Even though one does not expect the dissipation-dominated dynamics to last for long (due to the $1/\tau$ dependence of the dissipation term), one also must consider quantum and thermal fluctuations along with the motion of the front so that phase conversion can be achieved in a finite time even in large-volume limit. To have competing timescales, relevant fluctuations will necessarily be localized, possibly bubble like. In fact, even our assumption of uniformly varying profile of the order-parameter field has to be supplemented with presence of fluctuating modes of the field with shorter wavelengths on top of such a front. It is entirely possible that, for such a *fluctuating* front, incorporating short-wavelength modes, new *faster* timescales may emerge where the fluctuation parts may grow rapidly. All such issues need to be explored further and we intend to follow up this work with such investigations. However, in this first exploratory, study, we only focus on the slow-moving propagating front, which is just like a first-order interface, when there is no metastable vacua. Our results should then be taken in the spirit that the the dynamics of phase conversion may have much more richness, partly involving features of a first-order transition by the motion of interfaces even when there is no metastable vacua.

4.2.2 Numerical Solution

We calculate numerical solutions for the full Eq.(4.1), retaining the $\ddot{\phi}$ term. To correspond to the analytical solution, we first consider a large, constant, value of $\eta = (1/0.14)fm^{-1}$ in Eq.(4.1) (even though chiral transition occurs late at $\tau \simeq 4$ to 5 fm), and a uniform fixed $T = 150$ MeV. Note that this does not represent realistic QGP evolution in RHICE. We first study equations with constant (and uniform) T *only* to show exact correspondence with traditional reaction-diffusion equations. We will see that the resulting propagating front is exactly the same as that discussed in the literature for reaction-diffusion equations. Subsequently we relax this assumption of constant T and study the proper time-dependence of T for expanding QGP. We still retain the assumption of uniform temperature for studying front propagation because with spatially varying T the effective potential also has to vary spatially and correspondence with reaction-diffusion equation becomes remote. We consider the 1D case as suitable for the Newell-Whitehead equation. This will be applicable when the size of the traveling front is large, so a planar approximation can be used. Fig.4.1b gives the numerical profiles of the front $\phi(z)$ at different times (with initial time taken as 4 fm). The front starts at a distance of about 10 fm from the center and moves inwards converting the central region to the chiral-symmetry-broken phase. Note that, as T_0 everywhere has a value corresponding to the symmetry-broken phase, one would have expected a rapid roll down of the field to $\phi = \xi$ everywhere on a time of the order of 1 fm. In complete contrast to this, we see that phase conversion here happens slowly, by the motion of well defined interface, just as for the case of a first-order phase transition. As for Fig.4.1a, we obtain v here also directly from the traveling front. We find v ranging from 0.41 to 0.35, in close agreement with the

expected value $v = \frac{3m(T)}{\eta\sqrt{2}}$ $(= 0.42)$. By finding propagating solutions for different values of η we have verified (for both cases, Fig.4.1a, and Fig.4.1b) that the velocity of the front exactly scales as $1/\eta$.

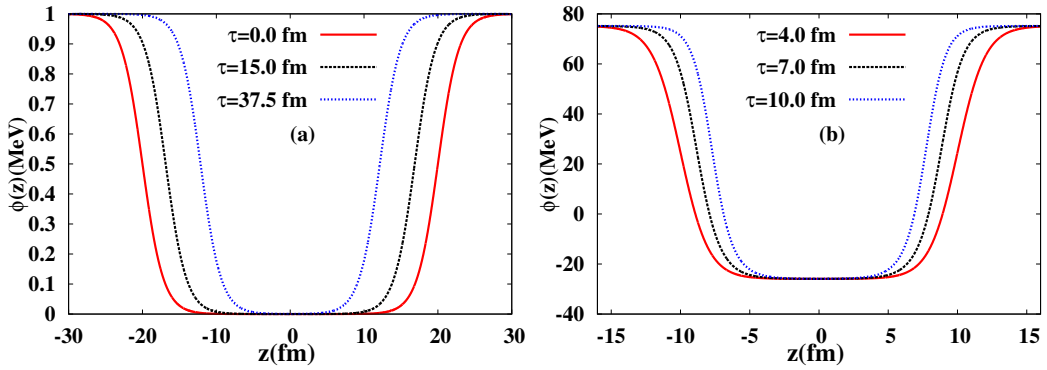

Figure 4.1: (a) Plots of the numerical solution for the traveling front of Eq.4.2 (as discussed in the text) at different times. Note that the form of propagating front solution of equation (4.3) corresponds to the profile of the front on the left part (negative z) in (a), with the origin selected at the midpoint of the left profile. (b) shows the numerical solution for the profile in Eq.(4.5) with nonzero H.

The propagating-front solutions we obtain are very robust and are almost independent of the initial profile of the front. To show this, we show the evolution of a profile consisting of linear segments (with correct boundary conditions) in Fig.4.2a. We see that this also develops into a well-defined propagating front as shown in Fig.4.1. Next, we consider realistic values of the time dependent $\eta = 1/\tau$ so that the second time-derivative term becomes important, with the initial value of $\tau = \tau_0 = 4.0$ fm, as appropriate for the chiral transition. We also take $T(\tau) = T_0(\tau_0/\tau)^{1/3}$ in accordance with Bjorken's scaling solution for the longitudinally expanding plasma. Fig.4.2b shows the traveling front solution for this case at different values of proper time τ. The only minor difference with the plots in Fig.4.1 is seen at somewhat later stages, with a little rise at the boundary of the front. The central value of ϕ changes in accordance with time-dependent T. It is clear that, with the presence of this *front* structure, for most of the results for first-order transition, such as nontrivial quark scattering, well defined phase-separated regions, fluctuations etc. will become applicable.

For Bjorken's 1D longitudinally expanding plasma, one should consider transverse motion of the front. Neglecting transverse expansion of the plasma, one should use Eq.(4.1) with cylindrical coordinates, or spherical expansion for the late stages of plasma evolution. Eq. (4.1) for these cases becomes

$$\ddot{\phi} - \frac{d^2\phi}{dr^2} - \frac{d-1}{r}\frac{d\phi}{dr} + \eta\dot{\phi} = -4\lambda\phi^3 + m(T)^2\phi + H, \tag{4.6}$$

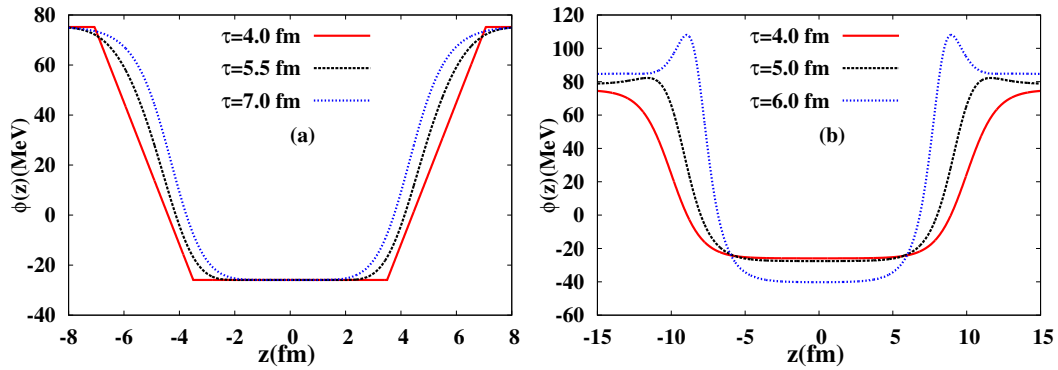

Figure 4.2: (a) Initial profile consisting of linear segments also rapidly evolves into a well-defined propagating front as in (a). (b) Solutions of Eq.(4.1), with realistic values of time-dependent η and time-dependent T.

where $d = 2$ for Bjorken's 1D longitudinal expansion, and $d = 3$ for spherical expansion. We have obtained front solutions for both these cases here for the chiral-symmetry case as well as later for the Z(3) case of C-D transition. The resulting solutions are very similar to those obtained for 1D case (as in Figs.4.1,4.2). Hence we do not show those plots.

4.3 Reaction-Diffusion Equation for Confinement-Deconfinement Transition

We now consider the case of confinement-deconfinement transition during the early thermalization stage. For RHICE, for very early stages, Bjorken scaling with longitudinally expanding plasma is a very good approximation. The dissipation term is very strong during the very early stages which helps in making a direct correspondence with reaction-diffusion equations. Because the traveling-wave solutions exist in the symmetry-broken phase we consider the case of the initial confinement-deconfinement transition using the Polyakov-loop order parameter with center symmetry Z(3) spontaneously broken in the high-temperature QGP phase. This early stage actually represents a nonequilibrium stage, with the system thermalizing to a maximum temperature T_0 in a timescale τ_0. The thermalization timescale τ_0 can be as short as about 0.14 fm (at LHC). Elliptic flow measurements indicate an upper bound of about 1 fm for τ_0. For the dynamics of the order parameter $l(x)$ which is the expectation value of the Polyakov loop, we use the following effective Lagrangian density [7].

$$L = \frac{N}{g^2}|\partial_\mu l|^2 T^2 - V(l), \tag{4.7}$$

Where the effective potential $V(l)$ for the Polyakov loop, in case of pure gauge theory, is given as

$$V(l) = (\frac{-b_2}{2}|l|^2 - \frac{b_3}{6}(l^3 + (l^*)^3) + \frac{1}{4}(|l|^2)^2)b_4T^4. \tag{4.8}$$

At low temperature where $l = 0$, the potential has only one minimum. As temperature becomes higher than T_c the Polyakov loop develops a nonvanishing vacuum expectation value l_0, and the $l^3 + l^{*3}$ term above leads to $Z(3)$-generated vacua. Now in the deconfined phase, for a small range of temperature above T_c, the $l = 0$ extremum becomes the local minimum (false vacuum) and a potential barrier exist between the local minimum and the global minimum (true vacuum) of the potential. Because we are interested in showing the existence of traveling front solutions in the absence of any first-order transition, we consider the value of the temperature T to be sufficiently large so that there is no such barrier present. For the parameter values we use, this requires $T > 280$ MeV, and we take $T = 500$ MeV. The values of various coefficients in Eq.(4.8) are the same as used in our previous works [8, 9] (including discussions about the explicit symmetry-breaking strength b_1) and we do not repeat that discussion here. (With those values of parameters, the transition temperature is taken to be $T_c = 182$ MeV.)

For simplicity we neglect the effect of dynamical quarks which lead to explicit breaking of Z(3) symmetry, and hence a linear term in l in $V(l)$ above [9]. This can be taken care of in a similar manner as for the explicit symmetry-breaking term H for the chiral symmetry case in Eq.(4.1). Similarly, because our interest is not in the Z(3) structure of the vacuum, we take l to be real. We again first neglect the second-order time derivative (for the large-dissipation case). The variables are scaled as $x \to gT\sqrt{\frac{b_4}{2N}}x$, and $\tau \to \frac{b_4 g^2 T^2}{2\eta N}\tau$. With that, the field equation for (real) $l(x)$ can be written as follows (for the sake of uniformity, we denote $l(x)$ as $\phi(x)$ in the following):

$$\dot{\phi} = \bigtriangledown^2\phi + \phi(b_2 + b_3\phi - \phi^2). \tag{4.9}$$

The final equation in this case is again a reaction-diffusion equation known as the Fitzhugh-Nagumo equation which is used in population genetics [3, 4]. Thus we again expect well defined traveling wave solutions for appropriate boundary conditions.

4.4 Propagating Front Solutions for Confinement-Deconfinement Transition

The required boundary conditions for the propagating front solution for Eq.(4.9) again naturally arise in RHICE, during early stages. As the system thermalizes, one expects first the center of the plasma to reach a temperature $T > T_c$ where T_c is the C-D transition temperature. The temperature in (somewhat) outer regions remains

below T_c initially. This leads to a profile of $l(x)$ where $l = 0$ in the outer regions while $l = 1$ at the center of the plasma. Subsequently, even these regions, somewhat away from the center, also achieve $T > T_c$. With these boundary conditions, we solve equations for $l(x)$ with a uniform temperature T with an initial value = 500 MeV. Eq.(4.9) above was derived in the large-dissipation limit to identify it with the Fitzhugh-Nagumo equation which guarantees the existence of a traveling wave solution for $l(x)$. With that assurance, we solve the full field equations for $l(x)$ (i.e. for $\phi(x)$) including the second time-derivative term. The dissipation term is naturally large initially in this case due to the $1/\tau$ factor with τ_0 being very small. Again, to show direct correspondence with reaction-diffusion equation, we take a very large, fixed value of $\eta = 1/\tau_0'$ with $\tau_0' = 0.01$ fm, and keep a fixed temperature value of $T = T_0 = 500$ MeV.

Plots in Fig.4.3a show the well-defined traveling wave solution at different values of τ starting from the initial time which is taken as $\tau_0 = 0.14$ fm. The initial profile is taken to have a similar form as in Fig.4.1, suitably modified for the boundary conditions appropriate for the present case. We next consider realistic value of time dependent $\eta = 1/\tau$ with initial value of $\tau = \tau_0 = 0.14$ fm, and take $T(\tau) = T_0(\tau_0/\tau)^{1/3}$ as appropriate for the Bjorken 1D scaling solution. The resulting evolution of $\phi(z)$ is shown in Fig.4.3b. Although ϕ shows some oscillations, it still shows a reasonably well defined propagating front. It is possible that η may not decrease as fast as $1/\tau$ due to presence of other sources of dissipation. In that case the resulting solution will be closer to that in Fig.4.3a.

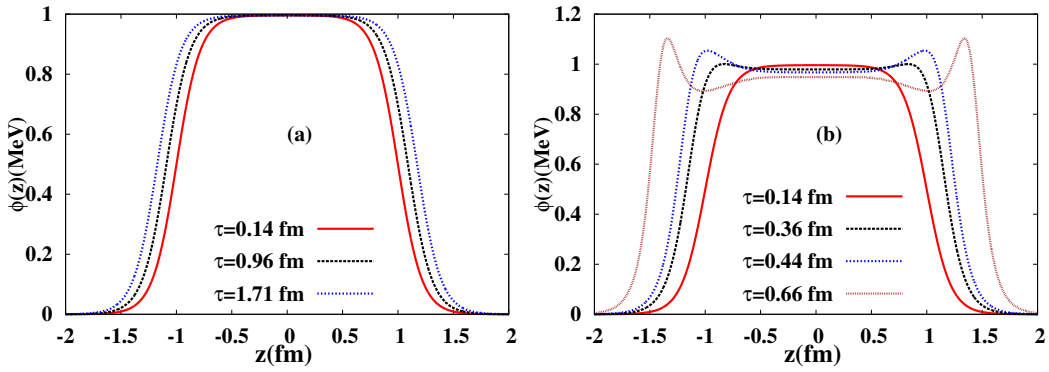

Figure 4.3: (a) Traveling wave solution for the Polyakov loop order parameter at different times for very large dissipation case with constant $\eta = 1/(0.01\text{fm})$. (b) Solution for realistic $\eta = 1/\tau$ and with time dependent T.

4.5 Relation Between Chiral Transition and Deconfinement Transition

We now address an important issue regarding the difference in the behavior of order-parameter evolutions for the chiral symmetry case and for the Polyakov loop for the C-D transition case. Note that we discussed the traveling wave solution for the chiral-symmetry case during late stages of the evolution, even though the presence of the large-dissipation case was harder to justify for such late stages ($1/\tau$ factor being relatively smaller). Similarly, for the early thermalization stage, we only discussed the case of the C-D transition with the Polyakov loop, and did not discuss the chiral-symmetry case. The reason is that the traveling-front solutions via the reaction-diffusion equation approach arise only when the effective potential has a specific shape; for example, that corresponding to spontaneous symmetry breaking. Thus, spontaneous breaking of Z(3) symmetry during early thermalization leads to well-defined traveling front for the Polyakov loop. But during this stage, chiral symmetry is restored. There is absolutely no possibility of finding any traveling-wave solution for the symmetry-restored effective potential for the chiral field ϕ (as one can simply check analytically as well as numerically). Similarly, while a traveling front exists for the chiral field during the chiral-symmetry-breaking transition during late stages of the plasma, there is no such solution for the Polyakov-loop order parameter at that stage because the Z(3) symmetry actually gets restored. This raises serious concerns about the conventional idea that the two transitions, namely the chiral transition and the C-D transition, are somehow related (or, are the same). In our calculations we clearly find regions separated by the traveling front of one order parameter whereas no such phase separation is expected from the other order parameter. Thus, we conclude that our results support the claims of several groups that the chiral transition and the C-D transition are indeed separate and independent transitions. In fact, our results provide clearly-phase-separated regions (by the traveling front) which are, e.g. chirally symmetric but in a confined phase, or in a chiral-symmetry-broken phase but in the deconfined phase. However, we caution that all these conclusions neglect the presence of fluctuations. As we discuss above, short-wavelength fluctuations are expected to lead to a new *shorter* time scale. It is possible that such a mixed dynamics, with fluctuations as well as a propagating front, may make the dynamics of the two transitions much more similar, although it looks unlikely that the two dynamics will become exactly the same. That will be possible only if the effects of the propagating front is completely negligible compared to fluctuations.

4.6 Conclusions

We conclude by emphasizing that the techniques of the reaction-diffusion equation have been used here to show the existence of well-defined traveling-front solutions,

which are very similar to phase boundaries for a first-order transition case, even though the relevant QCD transitions here are of second order, or a cross-over. This allows the very exciting possibility of using earlier results that are valid for a first-order-transition case, such as the formation of strangelets, baryon concentration, fluctuations etc. for RHICE. During the time when dissipation dominates, we see that the transition proceeds by a slow moving front, and may take several fm time to complete, leading to a long-lasting mixed-phase stage. This will affect calculations of various signals of QGP for RHICE, e.g. the production of thermal photons and dileptons, J/ψ suppression, and especially elliptic flow which develops mostly during the early stages. As we mentioned above, the reaction-diffusion equations have other solutions also with different propagation speeds. For example, Eq.(4.2) also has a static solution of the form $tanh(z)$. If the initial density profile in RHICE leads to such a profile of $\phi(z)$ the transition will become stagnant.

We again emphasize that one must consider quantum and thermal fluctuations along with the motion of the front so that phase conversion can be achieved in a finite time even in the large-volume limit. Relevant fluctuations will be short wavelength modes, possibly bubble like. Even the uniformly varying profile of the order-parameter field should incorporate fluctuating modes of the field with shorter wavelengths on top of such a front. It is entirely possible that for such a *fluctuating* front, incorporating short-wavelength modes, new *faster* timescales may emerge where the fluctuation parts may grow rapidly. We hope to investigate these issues in the future. Even with these concerns, it is clear that the possibility of a well-defined front governing at least partly the transition dynamics, will bring new richness to the transition dynamics in heavy-ion collisions. This will have important implications for RHICE. It is clearly of great importance to see if these results can be applied to the case of the early universe (for example, solutions with different speeds, especially the one with zero speed). The required initial boundary condition of $\phi = 0, 1$ for $x \to \pm\infty$ looks difficult to justify for the universe (due to absence of a temperature profile, as for RHICE). However, one should remember that there are always density (and hence temperature) fluctuations present in the universe (most likely of inflationary origin). Alhough these are very tiny (one part in 10^5), if we consider these fluctuations when the temperature of the Universe is very close to the transition temperature T_c then there can easily be regions of space where the symmetry is restored, while other neighboring regions will have a symmetry-broken phase.

This will lead to the required boundary conditions for the traveling wavefronts as discussed here. A small magnitude of temperature fluctuations will imply a small difference in the magnitude of Φ at the two boundary points, subsequently leading to small effects (like scattering of quarks). However,the typical wavelength of these fluctuations will be comparable to the Hubble size, naturally leading to wavefront propagation over such large scales. Thus, even with small quark scattering, etc., one may be able to get a large concentration of baryons via Witten's mechanism of nugget formation.

One caveat in this scenario is that chiral symmetry (as well as Z(3) symmetry) are

also explicitly broken. This makes the above-mentioned scenario difficult to implement for the quark-hadron transition when temperature fluctuations have very small magnitude. There may be other possibilities for the quark-hadron transition which we intend to explore in future work. However, such a mechanism will certainly apply to the electroweak phase transition where there is no explicit symmetry breaking involved. There also, one will get traveling front solutions arising from inflationary fluctuations irrespective of the order or of the strength of the phase transition. It will be interesting to investigate how such front solutions can affect the physics of post-electroweak transition physics, in particular sphaleron mediated baryogenesis, etc.

Bibliography

[1] E. Witten, Phys. Rev. **D 30**, 272 (1984).

[2] S. Digal and A.M. Srivastava, Phys. Rev. Lett. **80**, 1841 (1998).

[3] A.G. Nikitin, T.A. Barannyk, Central European Journal of Mathematics 2(5), 840 (2004); B. Bradshaw-Hajek, *Reaction-diffusion equations for population genetics*, PhD thesis, School of Mathematics and Applied Statistics, University of Wollongong, 2004, http://ro.uow.edu.au/theses/201;

[4] *Progress in Nonlinear Differential Equations and Their Applications*, Editor H. Brezis, Springer Basel AG, Switzerland (2004).

[5] R. Peschanski, Phys. Rev. **D**, 81, 054014 (2010); S. Munier and R. Peschanski, Phys. Rev. Lett. **91**, 232001 (2003); D. Ghoshal, JHEP, **1112**, 015 (2011); D. Ghoshal and P. Patcharamaneepakorn, JHEP, **1403**, 015 (2014).

[6] D. Boyanovsky, H. J. de Vega, R. Holman, and S. Prem Kumar, Phys. Rev. **D 56**, 3929 (1997).

[7] O. Scavenius, A. Dumitru, and J. T. Lenaghan, Phys. Rev. **C66**, 034903 (2002); R.D. Pisarski, Phys. Rev. **D62**, 111501R (2000).

[8] U. S. Gupta, R. K. Mohapatra, A. M. srivastava and V. K. Tiwari, Phys. Rev.**D82**, 074020 (2010).

[9] U. S. Gupta, R. K. Mohapatra, A. M. srivastava and V. K. Tiwari, Phys. Rev. **D 86** 125016 (2012).

Chapter 5

Possibility of DCC Formation in pp Collisions at LHC Energy via Reaction-Diffusion Equation

In the preceding chapter we saw how the application of reaction-diffusion equations to QCD phase transitions opens a new window on the dynamics of phase transitions. This chapter explores the possibility of DCC formation in pp collisions at LHC energy via reaction-diffusion equation. To that end, we first give a brief motivation behind our work. Sec. 5.1 reviews the basic physics of reaction diffusion equations where we discuss that the dynamics of chiral order parameter for chiral symmetry breaking transition with dissipative dynamics is governed by one such equation, specifically, the Newell-Whitehead equation [1]. Sec.5.2 discusses the basic physics of our model and Sec.5.3 presents results for the DCC formation. Conclusions are presented in section 5.4.

Some years ago there was a lot of interest in exploring the very interesting possibility that extended regions, where the chiral field is misaligned from the true vacuum, may form in large multiplicity hadronic collisions or in heavy-ion collisions [2–5]. Such a region was called a disoriented chiral condensate (DCC). A large DCC domain would lead to spectacular signatures such as coherent emission of pions which can be detected [3] as anomalous fluctuations in the ratio R of neutral pions to all pions. Original motivation for DCC came from Centauro events in cosmic ray experiments [3, 6]. However, even after intensive experimental searches for DCC, no clear signals for its formation were found. Alhough it was generally agreed that in heavy-ion collisions, chiral symmetry breaking transition will necessarily lead to formation of many DCC domains, the expected size of such DCC domains was too small, and their numbers were too large in any given event, that standard DCC signals were washed out. Indeed, from this perspective, heavy-ion collisions were not ideally suited for the detection of DCC. With a large volume system undergoing chiral symmetry

breaking transition, multiple DCC domains necessarily result, and a clean signal of coherent pion emissions becomes very unlikely. In comparison, a pp collision, with a small volume system, could, in principle, lead to a single DCC domain.

We revisit the issue of formation of DCC, this time in the context of (very) large multiplicity pp collisions at LHC energies. Some of the earliest suggestions for DCC formation were actually made in the context of high multiplicity hadronic collisions. One would expect that a pp collision, with a small volume system, could lead to a single DCC domain with a relatively cleaner signal of coherent pion emission. However, at previously attained energies, it was never clear whether the necessary condition for DCC formation, namely intermediate stage of chiral symmetry restoration, was ever achieved. Further, even if chiral symmetry was restored, the resulting DCC domains would have been too small of the order of a few fm^3, in view of rapid roll down of the chiral field to the true vacuum. This will lead to only few pions from which a clear signal, say of neutral to charged particle ratio, would be hard to detect.

The conditions of chiral symmetry restoration seem much more favorable for the very high multiplicity pp collisions at LHC energy. Indeed there are strong indications that several signals, such as flow, formation of ridge, etc. which have been attributed to a thermalized medium undergoing hydrodynamic expansion in heavy-ion collisions, may be present in such high energy pp collisions [7]. It is entirely possible that the energy density/temperature of such a medium may cross the chiral transition temperature. This will take care of the requirement of intermediate stage of chiral symmetry restoration for DCC formation. We show in this paper that the problem of rapid roll down of the chiral field to true vacuum is alleviated due to rapid three dimensional expansion of the system which makes reaction-diffusion equation applicable for governing the dynamics of chiral field for this system (with appropriate boundary conditions which, as we will show, naturally arise in these events). The expanding system leads to a DCC domain which stretches and becomes larger due to expansion, without the chiral field significantly rolling down (due to specific properties of the solutions of reaction-diffusion equations). Eventually one gets a large DCC domain whose subsequent decay should lead to coherent pion emission.

We will not attempt to give any arguments in the favor of chiral symmetry restoration in these high multiplicity pp events at LHC, and just refer the reader to the literature where evidence for the possibility of a thermalized medium in such collisions has been discussed [7]. We will only focus on the evolution of chiral field in such a system. Starting from a chirally symmetry phase (after some very early stage of rapid thermalization of partons produced in a central pp collision), a rapid three-dimensional expansion will quickly set in. This is due to the small size of the system resulting from pp collision, compared to heavy-ion collisions where the longitudinal expansion phase lasts for a significant time. The resulting rapid cooling of the system will lead to chiral symmetry breaking with the chiral field achieving some value in the vacuum manifold. With the explicit symmetry breaking term for the chiral effective potential being small, any value in the vacuum manifold will be (roughly) equally likely, leading to formation of a domain where chiral field is likely to be initially misaligned from

the true vacuum. This will be a DCC domain. Standard estimates for such a domain (from earlier investigations) lead to a typical size of coherence length of order 1 fm. The field will also roll down to the true vacuum rapidly in time of order few fm. It is very hard to detect such a DCC domain as this will lead to a very small number of coherent pions.

This is where the role of a reaction-diffusion equation becomes important. *Reaction-diffusion equations* [8–10], are usually studied for biological systems, e.g. population genetics, and chemical systems. Interestingly, a typical solution of such equations, with appropriate boundary conditions, consists of a traveling front with a well-defined profile, quite like the profile of the interface in a first order transition case [8–10]. This happens even when the underlying transition is a continuous transition or a crossover. In a previous work we have demonstrated that such *propagating front* solutions, separating the two QCD phases, exist for chiral phase transition and confinement-deconfinement (C-D) transition in QCD even when the underlying transition is a cross-over or a continuous transition [1]. We utilize the fact that the only difference between the field equations in relativistic field theory case and the reaction-diffusion case is the absence of a second order time derivative in the latter case. Thus, correspondence between the two cases is easily established in the presence of a strong dissipation term leading to a dominant first order time derivative term. Such a dissipative term arises due to plasma expansion in the form of the Hubble term. Further, we had argued that the required boundary conditions for the existence of such a *traveling front* naturally arise in the context of relativistic heavy-ion collision experiments (RHICE).

We extend that analysis [1] to the case of high multiplicity pp collisions at LHC energy. As we are interested in the formation of DCC, we focus here on the chiral transition. We argue that here also the appropriate boundary conditions which are suitable for the existence of propagating front solutions arise naturally. One important difference between the analysis in [1] and the present case is that previously we considered propagating front solutions separating chirally symmetric phase from the chiral symmetry broken phase. Here, in view of our focus on DCC formation, we consider the situation when the (approximate) chiral symmetry is spontaneously broken after an early stage of chiral symmetry restoration. We then consider the interior of the system to be such that the chiral field is *disoriented* there from the true vacuum, while it lies in the true vacuum outside. This constitutes the initial profile of the chiral field which gives the appropriate boundary conditions for the existence of propagating front solutions for the reaction-diffusion equation. We study the evolution of this profile as the system undergoes rapid 3D expansion. The other requirement for the applicability of the reaction-diffusion approximation to this case is the presence of strong dissipation. This is automatically satisfied due to a dissipation term (the Hubble term) arising from 3D spherical expansion (as well as due to coupling of the chiral field with other field modes).

We show that the propagating front solution *delays* the roll down of the chiral field in the interior of the region towards the true vacuum. At the same time rapid

expansion stretches the interior to a size of several fm radius before the field significantly rolls down towards the true vacuum. The resulting system constitutes a large, single, DCC domain which should lead to a relatively clear signal of coherent pion emission (e.g. in terms of the distribution of neutral to charged pion ratio).

We mention that in this work we have ignored the effects of thermal fluctuations. Such fluctuations are important and they will lead to some variations in the chiral field within a domain. However, in our model DCC formation results after chiral symmetry breakdown when the system undergoes a rapid 3D expansion, hence rapid cooling. Thus, presumably, thermal fluctuations will remain under control. The main point is that a large DCC domain is formed starting from a single small domain which stretches by rapid expansion and the only role thermal fluctuations can play is to fluctuate the field of this *single* DCC domain around the average *disoriented* value. These considerations have to be augmented with considerations of the quantum decay of the DCC domain into pions which will put a final limit on the growth of DCC domains in our model.

The chapter is organized in the following manner. Sec. 5.1 reviews the basic physics of reaction diffusion equations where we discuss that the dynamics of chiral order parameter for chiral symmetry breaking transition with dissipative dynamics is governed by one such equation, specifically, the Newell-Whitehead equation [1]. Sec.5.2 discusses the basic physics of our model and Sec.5.3 presents results for the DCC formation. Conclusion are presented in section 5.4.

5.1 Reaction-Diffusion Equation for Chiral Transition

There is a wide veracity of reaction-diffusion equations, see, e.g. ref. [8, 9]. We discussed earlier [1] specific equations which can be identified with the field equations for the chiral transition and the C-D transition in QCD in strong dissipation limit, leading to slowly moving propagating front solutions. We then showed that in different situations in relativistic heavy-ion collisions, with realistic dissipation, propagating front solutions of these equations still persist, making the dynamics of the relevant transitions effectively like a first order phase transition. Here, we will recall the case of chiral transition from ref. [1] and adopt it for the situation for the evolution of the field inside a DCC domain.

As we mentioned in the introduction, we will consider the case of high multiplicity pp collisions at LHC energy, assuming that the resulting partonic system undergoes a rapid 3D expansion. We take the field equations for the chiral field (from Eq.(2.25)) to be,

$$\ddot{\phi} - \bigtriangledown^2\phi + \eta\dot{\phi} = -4\lambda\phi^3 + m(T)^2\phi + H,$$

$$m^2(T) = \frac{m_\sigma^2}{2}(1 - \frac{T^2}{T_c^2}). \tag{5.1}$$

Here Φ is taken to be along the σ direction only which we represent by ϕ. This is for the sake of establishing a correspondence with the reaction-diffusion equation. Later, when we consider the case of DCC, we will consider other components of the chiral field Φ as well. In the above equation, the time derivatives are w.r.t the proper time τ. The dissipation term η is not a constant for expanding plasma. For the early stages in a heavy-ion collisions one normally takes Bjorken 1D scaling solution case with $\eta = 1/\tau$, which eventually turns into a 3D spherical expansion for which $\eta = 3/\tau$. For the present case of pp collision, due to small system size, one expects 3D expansion to be applicable from very early stages (after a time of order 1 fm). Hence, later on when we discuss the case of DCC, we will take $\eta = 3/\tau$.

Exact correspondence of the above equation with the reaction-diffusion equation was established in ref. [1] by neglecting the explicit breaking of chiral symmetry (i.e. $H = 0$ in Eq.(5.1)) and by considering the extreme dissipative case of a large, constant, value of η so that one could neglect the $\ddot{\phi}$ term. With rescaling of the variables as, $x \to m(T)x$, $\tau \to \frac{m(T)^2}{\eta}\tau$, and $\phi \to 2\frac{\sqrt{\lambda}}{m(T)}\phi$, the resulting equation is found to be,

$$\dot{\phi} = \bigtriangledown^2\phi - \phi^3 + \phi. \tag{5.2}$$

This equation, in one dimension with $\bigtriangledown^2\phi = d^2\phi/dx^2$, is exactly the same as the reaction-diffusion equation known as the Newell-Whitehead equation [8, 9]. In that context, the term $d^2\phi/dx^2$ is identified as the diffusion term while the other term on the right hand side of Eq.(5.2) is the so called *reaction term* (representing reaction of the members of a biological species for biological systems). Non-trivial traveling front solutions for the Newell-Whitehead equation arise with suitable boundary conditions, namely $\phi = 0$ and 1 at $x \to \pm\infty$. The analytical solution with these boundary conditions has the form,

$$\phi(z) = [1 + exp(z/\sqrt{2})]^{-1} \tag{5.3}$$

where $z = x - v\tau$. v is the velocity of the front [9] and has the value $v = 3/\sqrt{2}$ for this solution.

One can see from the general form of these reaction-diffusion equations, that such traveling front solutions will exist when the underlying potential allows for a nonzero order parameter in the vacuum state, along with a local maximum of the potential [8, 9]. The corresponding values of the order parameter provide the required boundary conditions for the propagating front solution. In ref. [1] we were interested in the dynamics of chiral-symmetry-breaking transition, hence we considered the two boundary values of the chiral field to be the true vacuum value and the one corresponding to the central maximum of the potential, respectively. For the case with a non-zero value of H as in Eq.(5.1), the value of the chiral field at one boundary was taken to be the (true) vacuum expectation value $\phi = \xi$ while the other boundary field value corresponded to the shifted central maximum of the potential $\phi = \phi_0$

(see, Fig.2.1). The propagating front solution in Eq.(5.3), suitably modified for these changed boundary conditions is [1],

$$\phi(z) = -\frac{(\xi - \phi_0)}{A_0}[1 + exp(\frac{m(T)(|z| - R_0)}{\sqrt{2}})]^{-1} + \xi, \tag{5.4}$$

where the normalization factor $A_0 = [1 + exp(\frac{-m(T)R_0}{\sqrt{2}}]^{-1}$. Here, we have restored the original, unscaled, variable z. $|z|$ was used in order to have a symmetric front on both sides of the plasma for the 1D case with R_0 representing the width of the central part of the plasma. For the 3D case, $|z|$ is replaced by the radial coordinate r. (Also, for the present case of pp collisions, we will multiply $m(T)$ by 3 to represent a sharper variation of ϕ initially. Note, this will be just a suitable choice of initial profile and a proper solution of a propagating front will result quickly when the initial profile is evolved by the field equations.)

In ref. [1] we calculated numerical solutions for the full Eq.(5.1), retaining the $\ddot{\phi}$ term. Correspondence with the analytical solution was achieved by considering a large, constant, value of η which resulted in propagating fronts of the same form as discussed in the literature for reaction-diffusion equations. Subsequently we relaxed this assumption of constant T and studied proper time dependence of T and η for expanding QGP (still retaining the assumption of uniform temperature for studying front propagation as with a spatially varying T the effective potential also has to vary spatially and correspondence with the reaction-diffusion equation becomes more complicated). We showed that the propagating front solution still exists with little modifications.

5.2 DCC Formation via the Reaction-Diffusion Equation

In the present work we are considering the situation of the evolution of the *disoriented* chiral field after chiral symmetry breaking transition. We recall the picture of DCC from Chapter 2 where we discussed that a DCC corresponds to a physical region in the interior of which the chiral field is disoriented from the true vacuum. Thus the two boundary conditions for the propagating front solution have to be appropriately modified. The basic picture of DCC formation in this case will be taken as follows. In a high multiplicity pp collision, we will assume that a thermalized medium is created and that temperature/energy density of this medium reaches a sufficiently large value so that the (approximate) chiral symmetry is restored during very early stages. Due to the very small size of the initial system, it undergoes a 3D spherical expansion after a very short time of order 1-2 fm. This leads to a rapid cooling of the system and the chiral symmetry is spontaneously broken. This is the starting point of our calculation, with the initial profile of the chiral field in the interior of the system assuming some arbitrarily chosen value on the (approximately degenerate) vacuum

manifold. We will consider the case of maximal disorientation when the field in the center of the parton system takes the value at the saddle point *opposite* to the true vacuum on the vacuum manifold. Outside the system the chiral field was always in the true vacuum and we assume that it continues to have values close to the same value in somewhat interior regions as well (where the temperature could be taken to develop a similar value as the central temperature). This sets the two boundary conditions for the initial profile of the chiral field and we study whether an initial profile with such boundary conditions can lead to a propagating front solution. (We mention that for the sake of numerical integration of the differential equation, we need to fix the boundary conditions at $r = 0$ and for large r. However, the initial profile taken has a plateau for small r; hence the field is allowed to roll down freely in the region away from $r = 0$. Indeed, such a profile with the same boundary conditions shows rapid roll down for the symmetry restored potential where one does not expect any propagating solution. Also, for one dimensional case, we consider the chiral field to have a symmetric profile about $x = 0$ and the boundary conditions are only fixed for large $|x|$ with the $x = 0$ point free to evolve via the differential equation. Exactly same results of propagating front solution are still obtained on both sides of $x = 0$.)

The profile of the chiral field in between the two boundary values (as discussed above) is taken to lie on the vacuum manifold and we choose this profile, for simplicity, to remain in the $\sigma - \pi_3$ plane. In such a DCC domain, the decay of the field will lead to emission only of neutral pions. If we had chosen the field to remain in any plane of (π_1, π_2, σ), it would lead to emission only of charged pions. For a more general possibility, appropriate distribution of neutral and charged pions will be obtained.

Note that it is not immediately obvious that such boundary conditions should lead to a propagating front solution. For reaction-diffusion equations, the corresponding boundary condition is set for a local maximum of the potential, and not for a saddle point. However, it appears that the importance of the maximum of the potential is in delaying the roll-down of the field from that point due to vanishing field derivative. In that situation, a saddle point will also satisfy this requirement and a propagating front solution should result. As we will see, this intuition seems correct and we do find propagating solutions with this new type of boundary conditions. We have checked that if the field at that boundary is taken even close to the saddle point (say, within 10-20 %), slowly propagating front still results and our results remain essentially unaffected.

For the present case of 3-dimensional expansion, with spherical symmetry, will use the field equations in spherical polar coordinates,

$$\ddot{\Phi}_i - \frac{d^2\Phi_i}{dr^2} - \frac{2}{r}\frac{d\Phi_i}{dr} + (\frac{3}{\tau} + \eta'(T))\dot{\Phi}_i = -4\lambda|\Phi|^2\Phi_i + m(T)^2\Phi_i + H\delta_{i4}, \tag{5.5}$$

where Φ_i denote components of the O(4) vector Φ. For this 3-dimensional expansion case, the temperature is taken to vary with proper time as,

$$T(\tau) = T_0\frac{\tau_0}{\tau}. \tag{5.6}$$

The initial value of the temperature for field evolution is taken to be $T = T_0 = 150$ MeV, at proper time $\tau = \tau_0 = 2$ fm. This stage corresponds to chiral symmetry broken phase. The system is assumed to have reached a value larger than the critical temperature at an earlier stage which allows for the chiral field to become disoriented after the transition. Here, we have introduced a new dissipation parameter $\eta'(T)$, in addition to the Hubble damping coefficient $3/\tau$ [11, 12]. η' represents dissipation due to coupling to the heat bath, or due to other field modes (which could be fields other than the chiral field, or even high frequency modes of the chiral field itself). The value of this dissipation parameter has been discussed in the literature (see, e.g. ref. [11,12] and references therein). We mention that inclusion of η' is not essential in our model of DCC formation as Hubble damping itself can be very large at sufficiently early times. However, from general considerations, one will always expect such an additional damping, and it certainly helps for getting a slow moving propagating front leading to a large DCC domain. We first take $\eta' \propto T^2$ with the initial value of $\eta' = 10$ fm $^{-1}$ at $\tau = \tau_0$. Subsequently, we will also consider the case with a constant, time independent, $\eta' = 20$ fm^{-1} and 40 fm^{-1}. We consider these larger dissipation cases to allow for the possibility of the chiral field coupling to other field modes, and to show that larger dissipation can lead to much larger increase in DCC domain size in this model.

5.3 Results

We now present the results of field evolution via Eq.(5.5). The initial profile of the chiral field, at $\tau = \tau_0 = 2$ fm, is shown in Fig.5.1a. The solid curve shows the profile of the σ field which interpolates between the true vacuum value $\sigma = 75.18$ MeV and the saddle point opposite to the true vacuum where $\sigma = -49.25$ MeV (with $\vec{\pi} = 0$ at both these boundaries). The interpolating profile of σ is taken in accordance with Eq.(5.4) (for the 3-dimensional case with radial coordinate r as discussed there), with ϕ_0 and ξ suitably replaced by the boundary conditions for the present case. Further, since the chiral field is taken to lie everywhere on the (approximately degenerate) vacuum manifold, hence the $\vec{\pi}$ field also varies in between the two boundary points, as shown by the dashed curve for π_3 in Fig.5.1a . This is fundamentally different from the case of chiral transition considered in our previous work where the pion field was taken to be zero all along the profile of σ which interpolated between the true vacuum and the central maximum of the potential. We again mention that the choice of the chiral field to lie entirely in the $\sigma - \pi_3$ plane is just an example. Such a DCC will decay by emitting neutral pions. One could take a more general variation, in which case an appropriate distribution of neutral and charged pions will result.

We have taken the radius of the system to be about 2.5 fm assuming that the initial dense parton system in the pp collision would have undergone some expansion by the time this stage is achieved at $\tau_0 = 2$ fm. This initial profile is evolved using Eq.(5.5). Note that Eq.(5.5) is written in comoving coordinates. As the system is

undergoing a 3D scale invariant expansion, the physical distances have to be obtained by multiplying with the appropriate scale factor. For this purpose we have taken the velocity of the plasma at a comoving distance r to be proportional to r, with some maximum velocity at the boundary of the region (which we take as a sample value to be 0.9). Plots at subsequent stages are shown in Figs.5.1b-d with the x axis denoting the physical distance. This is where we see the importance of the front solution of the reaction-diffusion equation. Normally one would have expected that the field from the saddle point will roll down towards the true vacuum in a time scale of a couple of fm within the whole system of size of 2-3 fm. However, the front solution delays this roll down dramatically. The field retains its value close to the saddle point in a significant region for a long duration of time (due to slow motion of the front).

During this period, the rapid expansion of the plasma stretches the whole system, thereby stretching the region where the chiral field is close to the saddle point, hence disoriented. This leads to a DCC domain which is expanding and getting bigger without the chiral field in the interior rolling down towards the true vacuum. This is shown in Fig.5.1b (for the σ field) and Fig.5.1c (for π_3). Note that the stretching of a DCC domain costs energy and this should be properly accounted for by calculating the back reaction of DCC stretching on the expanding plasma. However, for ultra relativistic pp collisions the expanding parton system will have very large kinetic energy, and the effects of back reaction of stretching of a DCC domain will not be significant for the time scales considered here. Fig.5.1b shows the σ field profile (dashed curve) at $\tau = 4$ fm clearly showing that the DCC domain (the region where the field is significantly disoriented from the true vacuum) has almost doubled in size. This means multiplication in the number of coherent pions by a factor of 8 (compared to the number expected from the DCC domain of initial parton system size) when the DCC eventually decays. Fig.5.1d shows the situation at $\tau \simeq 7.2$ fm when the chiral field has significantly rolled down towards the true vacuum. One can say that the decay of the DCC domain has set in by this stage. Eventually the DCC domain decays with the chiral field rolling down to the true vacuum.

We now consider case of larger dissipation with constant η'. Figs.5.2 a,b show the stages corresponding to the stages in Fig.5.1 b,c,d for the case with constant $\eta' = 20$ fm^{-1}. Figs.5.2 c,d show similar stages for constant $\eta' = 40$ fm^{-1}. We note significant increase in the stretching of DCC domains. In fact by $\tau = 7.2$ fm the fields have still not started significantly deviating from the disoriented value. We do not show plots for large τ because, as mentioned above, the decay of a DCC domain by thermal fluctuations as well as quantum effects will limit the growth of DCC domain. It is not clear if such large and (quasi) constant values of η' can be realistic. However, its significant effect on the formation of large DCC domains may be taken as a strong motivation for finding arguments/situations where such strong dissipation may be justified/applicable.

We showed in ref. [1] that the propagating front solutions we obtain are very robust and almost independent of the initial profile of the front taken. Thus our results obtained here are not very sensitive to the exact initial profile of the chiral

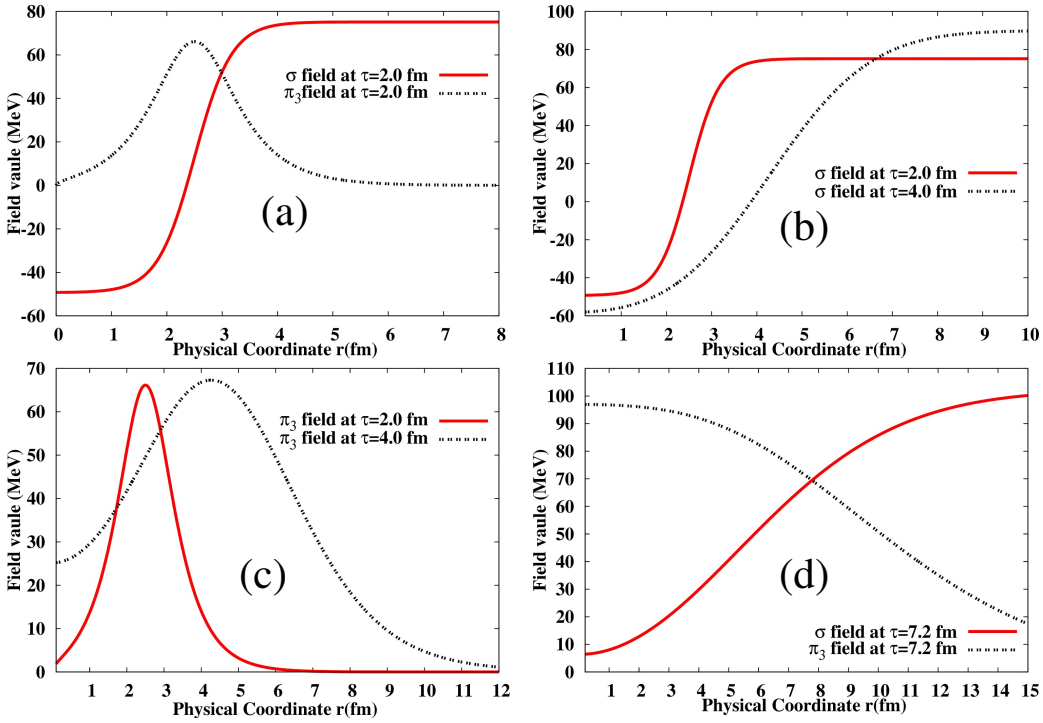

Figure 5.1: (a) The initial profile of the chiral field. Solid (red) curve shows the profile of the σ field which interpolates between the true vacuum value $\sigma = 75.18$ MeV and the saddle point opposite to the true vacuum where $\sigma = -49.25$ MeV. Corresponding variation of π_3, ensuring that the field (approximately) lies on the vacuum manifold, is shown by the dashed (black) curve. (b) Dashed (black) curve shows the profile of the σ field after the system has undergone expansion up to $\tau = 4$ fm. For comparison, solid (red) curve shows the initial σ profile. Stretching of the plasma leading to expansion of the DCC domain is clearly seen. (c) Corresponding profile of π_3 field at $\tau = 4$ fm is shown by the dashed (black curve), while the solid (red) curve shows the initial π_3 profile. (d) This shows the stage at $\tau \simeq 7.2$ fm when the decay of the DCC domain has set in with the chiral field significantly moving away from the initial disoriented value. Solid (red) and dashed (black) curves show, respectively, σ and π_3 field profiles.

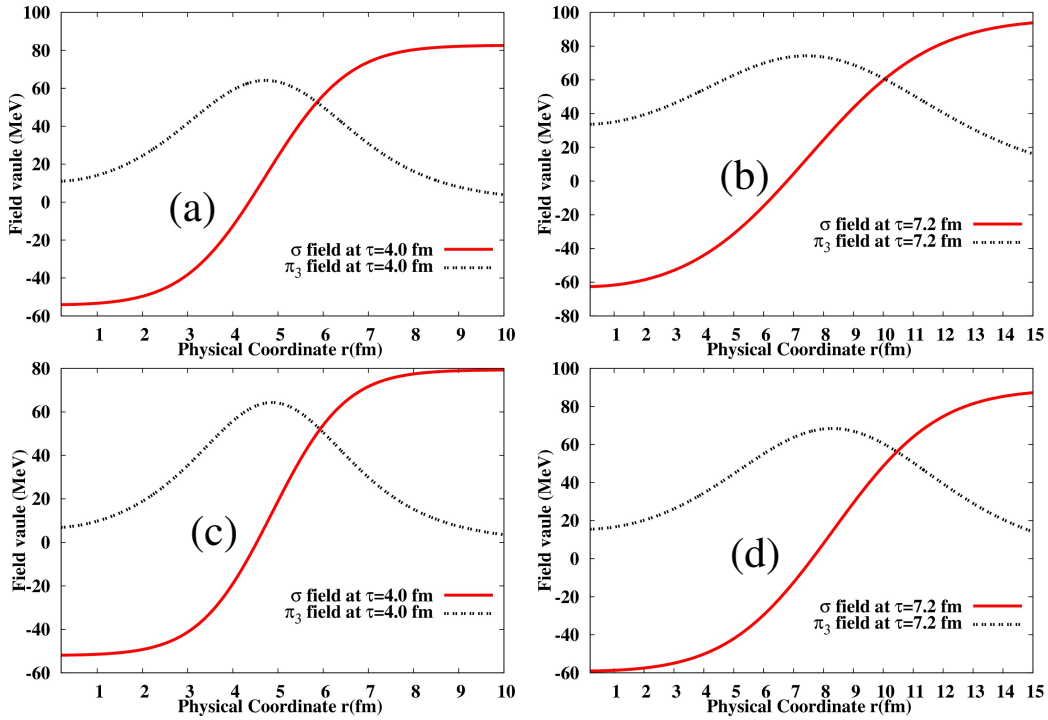

Figure 5.2: (a) and (b) show the profiles of the chiral field at the same stages as in Fig.5.1 b,c and Fig.2d (starting with the same initial profiles as in Fig.5.1a). η' is taken as constant for this case with the value 20 fm^{-1}. Comparison with Fig.5.1 shows that the DCC domain stretches to a much larger size in this case. (c) and (d) show similar stages as in (a) and (b), but now with even larger $\eta' = 40$ fm^{-1}. We see a much larger DCC domain resulting here.

field taken. A different profile would still lead to similar qualitative features of the evolution of the parton system and hence a DCC domain.

5.4 Conclusions

We conclude by pointing out the important features of our analysis. We focus on high multiplicity pp collisions at LHC energy as potentially important for possible formation of *single* DCC domains. This is in contrast to heavy-ion collisions where necessarily one gets multiple DCC domains where a clean signature of coherent pions becomes difficult to detect. The problem of small size for pp collision (hence small DCC domain) is circumvented by showing the existence of slowly moving fronts governed by reaction-diffusion equation. This delays the roll down of the disoriented chiral field to the true vacuum significantly, while the system undergoes a rapid three dimensional expansion. This leads to stretching of the initial DCC domain to a size of several fm which can lead to relatively clean signals of coherent pion emission.

The specific assumptions made in our model, such as the value of the dissipation constant, initial profile, etc. are not expected to significantly change the main aspects of our results. In view of our previous results in ref. [1], the existence of slowly moving propagating front results under varied conditions and with widely different initial profiles. This is in complete contrast to the usual expectation that the field should rapidly roll down to the true vacuum. Thus, high multiplicity pp collisions at LHC energy may be an ideal place to look for the long-sought signatures of disoriented chiral condensates. The considerations presented here are about classical evolution of the chiral field in an expanding domain. As we mentioned above, considerations of thermal fluctuations and quantum decay of the DCC domain into pions will put the final constraint on the growth of DCC domains in our model.

Bibliography

[1] P. Bagchi, A. Das, S. Sengupta, and A.M. Srivastava, Phys. Rev. **C92** (2015) 3, 034902.

[2] A. A. Anselm, Phys. Lett. **B217** (1989) 169; J.-P. Blaizot and A. Krzywicki, Phys. Rev. **D46** (1992) 246.

[3] J.D. Bjorken, K.L. Kowalski and C.C. Taylor, in *Results and Perspectives in Particle Physics 1993*; Proceedings of the 7th Rencontres de Physique de la Vallee d'Aoste, La Thuile, Italy, 1993, edited by M. Greco (Editions Frontieres, Gif-sur-Yvette, France, 1993).

[4] J. P. Blaizot and D. Diakonov, Phys. Lett. **B315** (1993) 226.

[5] K. Rajagopal and F. Wilczek, Nucl. Phys. **B399** (1993) 395; *ibid* **B404** (1993) 577.

[6] C. M. G. Lattes, Y. Fujimoto and S. Hasegawa, Phys. Rep. **65**, 151 (1980); L. T. Baradzei et al., Nucl. Phys. **B370**, 365 (1992), and references therein.

[7] P. Ghosh, S. Muhuri, J.K. Nayak, and R. Varma J.Phys. **G 41**, 035106 (2014); I.B. Bashir, R.A. Bhat, and S. Uddin, arXiv: 1502.04185.

[8] A.G. Nikitin, T.A. Barannyk, Central European Journal of Mathematics 2(5), 840 (2004); B. Bradshaw-Hajek, *Reaction-diffusion equations for population genetics*, PhD thesis, School of Mathematics and Applied Statistics, University of Wollongong, 2004, http://ro.uow.edu.au/theses/201;

[9] *Progress in Nonlinear Differential Equations and Their Applications*, Editor H. Brezis, Springer Basel AG, Switzerland (2004).

[10] R. Peschanski, Phys. Rev. **D**, 81, 054014 (2010); S. Munier and R. Peschanski, Phys. Rev. Lett. **91**, 232001 (2003); D. Ghoshal, JHEP, **1112**, 015 (2011); D. Ghoshal and P. Patcharamaneepakorn, JHEP, **1403**, 015 (2014).

[11] S. Digal, R. ray, S. Sengupta, and A.M. Srivastava, Int. J. Mod. Phys. **A 15**, 2269 (2000).

[12] T. S. Biro and C. Greiner, Phys. Rev. Lett. **79**, 3138 (1997); C. Greiner, Z. Xu and T. S. Biro, hep5-ph/9809461.

Chapter 6

Summary

Here we summarize the work presented in this thesis. We have applied the techniques of reaction diffusion equations to study various aspects of the dynamics of QCD transitions. The most important aspect of this approach originates from the existence of well defined propagating front solutions of reaction-diffusion equations which are very similar to phase boundaries in a first order transitions, even when the underlying transition is not a first order transition.

We first presented a brief review of QCD and the physics of QGP in Chapter 1, and then discussed different aspects of QCD phase transitions in Chapter 2, specifically, the chiral transition and the confinement-deconfinement (C-D) transition. We discussed the effective Lagrangians for these transitions. For the chiral transition we used the linear sigma model written in terms of the order parameter field Φ, which is an $O(4)$ vector. We provided a brief discussion of the physical picture of DCC formation. For the C-D transition, we used the effective Lagrangian for the thermal expectation value of the Polyakov loop which acts as an order parameter for the C-D transition. We then addressed the issue of the dynamics of transition for both these cases and briefly discussed the formation of QGP in relativistic heavy-ion collisions.

Earlier it used to be believed that the quark-hadron transition is of first order even at low chemical potential (as in the early universe). This had important implications as with quarks scattering from the expanding interfaces, separating the QGP phase from the hadronic phase, quark nuggets could form in the early universe which could serve as a candidate for dark matter of the universe. The dynamics of first order transition also had important implications for heavy-ion collisions. However, with lattice results showing the quark-hadron transition to be a cross-over, such possibilities became unrealistic, at least for the case of the universe and for ultra-relativistic heavy-ion collisions.

In view of the importance of interfaces for such important physical effects associated with a first order transition, we considered the possible role of reaction-diffusion equations for QCD transitions. This is because well formed, propagating interfaces routinely arise in the context of *reaction-diffusion equations* even when the underlying

transition is a continuous transition or a cross-over. We provided a brief review of reaction-diffusion equations in Chapter 3.

Chapter 4 and 5 present our research work. In Chapter 4 we demonstrated the existence of propagating front solutions for chiral phase transition and confinement-deconfinement (C-D) transition in QCD even when the underlying transition is a cross-over or a continuous transition. We utilized the fact that the only difference between the field equations in relativistic field theory case and the reaction-diffusion case is the absence of a second order time derivative in the latter case. The correspondence between the two cases was, thus, established in the presence of a strong dissipation term leading to a dominant first order time derivative term. We also showed that the required boundary conditions for the existence of such slowly moving propagating fronts naturally arise in relativistic heavy-ion collision experiments (RHICE).

In Chapter 5 we considered an important application of the reaction-diffusion-equation-governed dynamics of QCD transition. We investigated the issue of formation of disoriented chiral condensate (DCC). DCC corresponds to formation of an extended region, where the chiral field is misaligned from the true vacuum. This possibility was investigated extensively some time ago and it was proposed that DCC may form in large multiplicity hadronic collisions or in heavy-ion collisions. A large DCC domain would lead to spectacular signatures such as coherent emission of pions which can be detected as anomalous fluctuations in the ratio of neutral pions to all pions. However, even after extensive experimental search for DCC, no clear signals were found for its formation. Although it was generally agreed that in heavy-ion collisions, chiral-symmetry-breaking transition will necessarily lead to formation of many DCC domains, the expected size of such DCC domains was too small, and their numbers too large in any given event, that standard DCC signals were washed out. Indeed, from this perspective, heavy-ion collisions were not ideally suited for the detection of DCC. With a large volume system undergoing chiral symmetry breaking transition, multiple DCC domains necessarily result, and a clean signal of coherent pion emissions becomes very unlikely. In comparison, a pp collision, with a small volume system, could, in principle, lead to a single DCC domain.

We considered the issue of DCC formation in the context of (very) large multiplicity pp collisions at LHC energies. The conditions of chiral symmetry restoration seem favorable for the very high multiplicity pp collisions at LHC energy. We showed that the problem of rapid roll down of the chiral field to true vacuum is avoided due to a rapid three dimensional expansion of the system which makes reaction-diffusion equation applicable for governing the dynamics of the chiral field for this system (with appropriate boundary conditions which, as we will show, naturally arise in these events). The expanding system leads to a DCC domain which stretches and becomes larger due to expansion, without the chiral field significantly rolling down (due to specific properties of the solutions of reaction-diffusion equation). Eventually one gets a large DCC domain the subsequent decay of which should lead to coherent pion emission.

In conclusion, we have used the techniques of reaction-diffusion equations to show the existence of well defined traveling front solutions, which are very similar to phase boundaries for a first order transition case, even though the relevant QCD transitions here are of second order, or a cross-over. This will have important effects, especially on various signals of QGP. We considered one particular important implication of such fronts showing that it may lead to the possibility of formation of disoriented chiral condensates (DCC) in high multiplicity pp collisions at LHC energy.